Bull Volcanol (1999) 60: 381–401

ORIGINAL PAPER

M. C. Jackson · F. A. Frey · M. O. Garcia · R. A.Wilmoth

Geology and geochemistry of basaltic lava flows and dikes from the Trans-Koolau tunnel, Oahu, Hawaii

Received: 1 June 1998 / Accepted: 30 August 1998

Abstract A 200-m section of Koolau basalt was sampled in the 1.6-km Trans-Koolau (T–K) tunnel. The section includes 126 aa and pahoehoe lava flows, five dikes and ten thin ash units. This volcanic section and the physical characteristics of the lava flows indicate derivation from the nearby northwest rift zone of the Koolau shield. The top of the section is inferred to be 500–600 m below the pre-erosional surface of the Koolau shield. Therefore, compared with previously studied Koolau lavas, this section provides a deeper, presumably older, sampling of the shield. Shield lavas from Koolau Volcano define a geochemical end-member for Hawaiian shields. Most of the tunnel lavas have the distinctive major and trace element abundance features (e.g. relatively high SiO_2 content and Zr/Nb abundance ratio) that characterize Koolau lavas. In addition, relative to the recent shield lavas erupted at Kilauea and Mauna Loa volcanoes, most Koolau lavas have lower abundances of Sc, Y and Yb at a given MgO content; this result is consistent with a more important role for residual garnet during the partial melting processes that created Koolau shield lavas. Koolau lavas with the strongest residual garnet signature have relatively high $^{87}Sr/^{86}Sr$, $^{187}Os/^{188}Os$, $^{18}O/^{16}O$, and low $^{143}Nd/^{144}Nd$. These isotopic characteristics have been previously interpreted to reflect a source component of recycled oceanic crust that was recrystallized to garnet pyroxenite. This component also has high La/Nb and relatively low $^{206}Pb/^{204}Pb$, geochemical characteristics which are attributed to ancient pelagic sediment in the recycled crust. Although most Koolau lavas define a geochemical endmember for Hawaiian shield lavas, there is considerable intrashield geochemical variability that is inferred to reflect source characteristics. The oldest T–K tunnel lava flow is an example. It has the lowest $^{87}Sr/^{86}Sr$, Zr/Nb and La/Nb, and the highest $^{143}Nd/^{144}Nd$ ratio found in Koolau lavas. In most respects it is similar to lavas from Kilauea Volcano. Therefore, the geochemical characteristics of the Koolau shield, which define an end member for Hawaiian shields, reflect an important role for recycled oceanic crust, but the proportion of this crust in the source varied during growth of the Koolau shield.

Key words Koolau Volcano · Hawaiian shield lavas · Igneous geochemistry · Recycling of oceanic crust

Editorial responsibility: W. Hildreth

M. C. Jackson
Department of Earth and Planetary Sciences, McGill University, Montreal, Quebec, H3 A 2A7, Canada

F. A. Frey (✉)
Department of Earth, Atmospheric and Planetary Sciences, Massachusetts Institute of Technology, Cambridge, Massachusetts, USA
e-mail: fafrey@mit.edu

M. O. Garcia
Department of Geology and Geophysics, University of Hawaii, Honolulu, Hawaii, USA

R. A.Wilmoth
Columbia Geotechnical, P.O. Box 87367, Vancouver, Washington 98687, USA

Introduction

Koolau Volcano on the island of Oahu, Hawaii, is an unusual Hawaiian volcano in terms of its evolutionary history and geochemical characteristics. For example, the tholeiitic shield is not overlain by post shield-stage lava flows, but it has an areally extensive rejuvenated (post-erosional) stage (Honolulu Volcanics). In major and trace element composition and isotopic ratios (Sr, Nd, Pb, Os and O), the Koolau shield lavas define a geochemical end member for Hawaiian lavas (Stille et al. 1983; Roden et al. 1984, 1994; Frey et al. 1994; Eiler et al. 1996; Lassiter and Hauri, in press). Lavas from diverse parts of the Koolau shield and dikes from the caldera complex have these distinctive geochemical characteristics; therefore, there is no doubt that the source of studied Koolau lavas was geochemically different from the source of the currently active Hawaiian shields (Loihi, Kilauea and Mauna Loa). Although Koolau lavas show considerable isotopic heterogeneity, previous studies

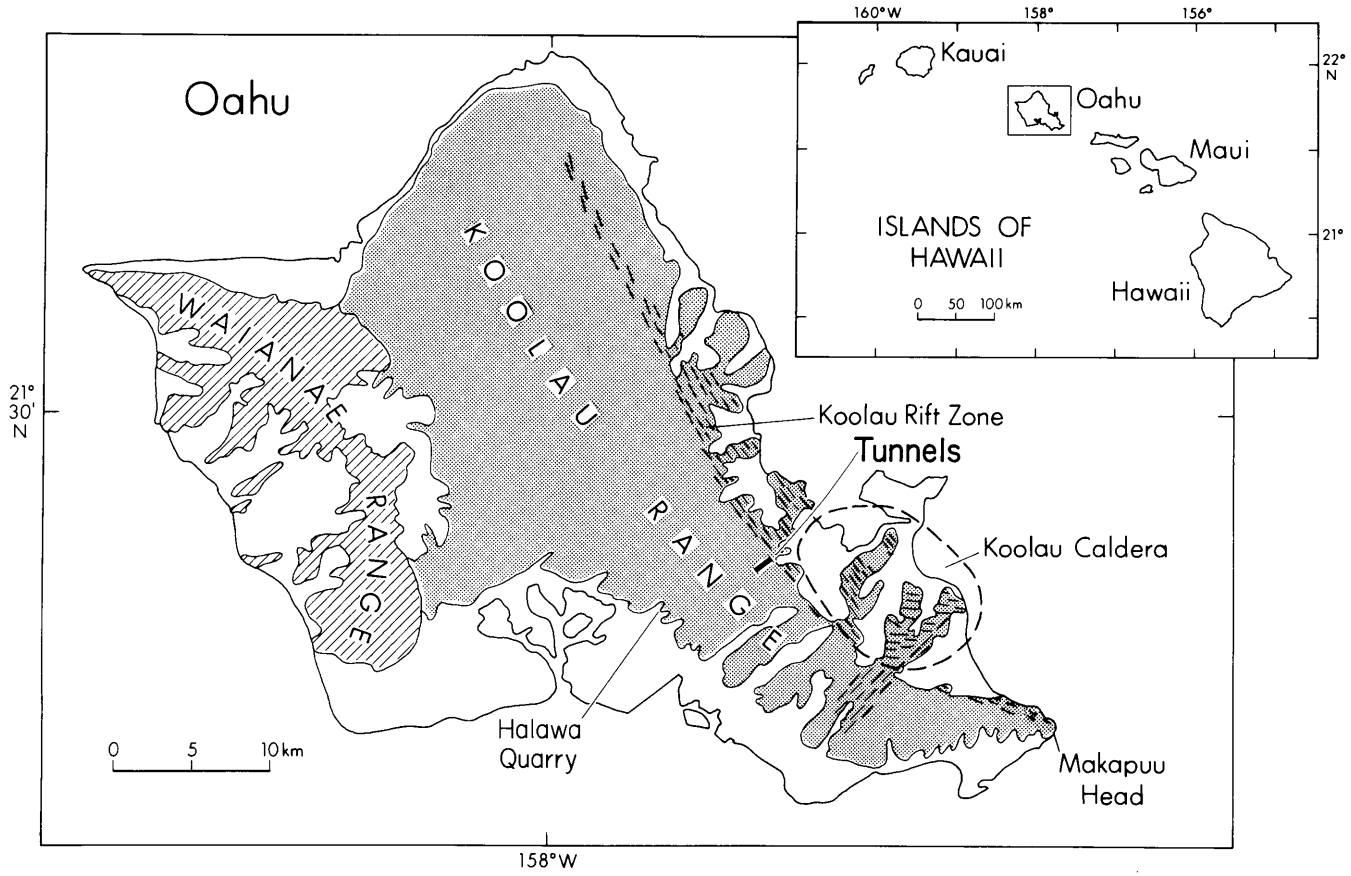

Fig. 1 Map of Oahu showing the Waianae and Koolau shields and locations of the Trans-Koolau tunnel, which extends southeastward from North Halawa Valley to Haiku Valley, the inferred Koolau caldera, the northwest rift zone, the Koolau dike complex (*dashed lines*), Makapuu Head and Halawa quarry. *Inset* shows location of Oahu relative to other Hawaiian islands

found no systematic geochemical variations with relative age of lavas in stratigraphic sections. This result contrasts with recent studies of Mauna Loa Volcano (Rhodes and Hart 1995; Kurz et al. 1995).

This article describes the stratigraphy, morphology, petrography and geochemistry of lava flows and dikes from a 200-m-thick section exposed in the 1.6-km-long Trans-Koolau (T–K) tunnel. The T–K tunnel sequence, dominantly lava flows with a few dikes and pyroclastic layers, is inferred to represent a near-vent facies derived from the nearby northwest rift zone. Relative to the Makapuu Head section of Koolau lavas studied by Frey et al. (1994) and Roden et al. (1994), the T–K tunnel section is closer to the paleo-caldera of the Koolau shield (Fig. 1), is deeper below the pre-erosional surface, and is presumably older. In an effort to further evaluate the temporal geochemical trends of Koolau lavas, one of our objectives was to compare the geochemical characteristics of the relatively old T–K tunnel lavas with Koolau lavas from other stratigraphic sections.

Geologic setting

The island of Oahu has two volcanoes (Fig. 1). The older one, Waianae Volcano of western Oahu, ~2.9–3.9 Ma (Doell and Dalrymple 1973; Presley et al. 1997), consists of a tholeiitic shield (Waianae Volcanics) overlain by flows of a

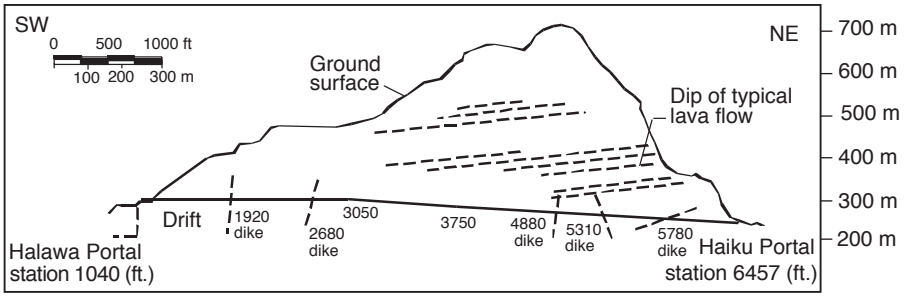

Fig. 2 Cross section through the Koolau range showing the regional dip of shield lavas, the location of the Trans-Koolau tunnel and locations of dikes intersected by the tunnel. *Numbers* (in feet) relate to originally surveyed distances

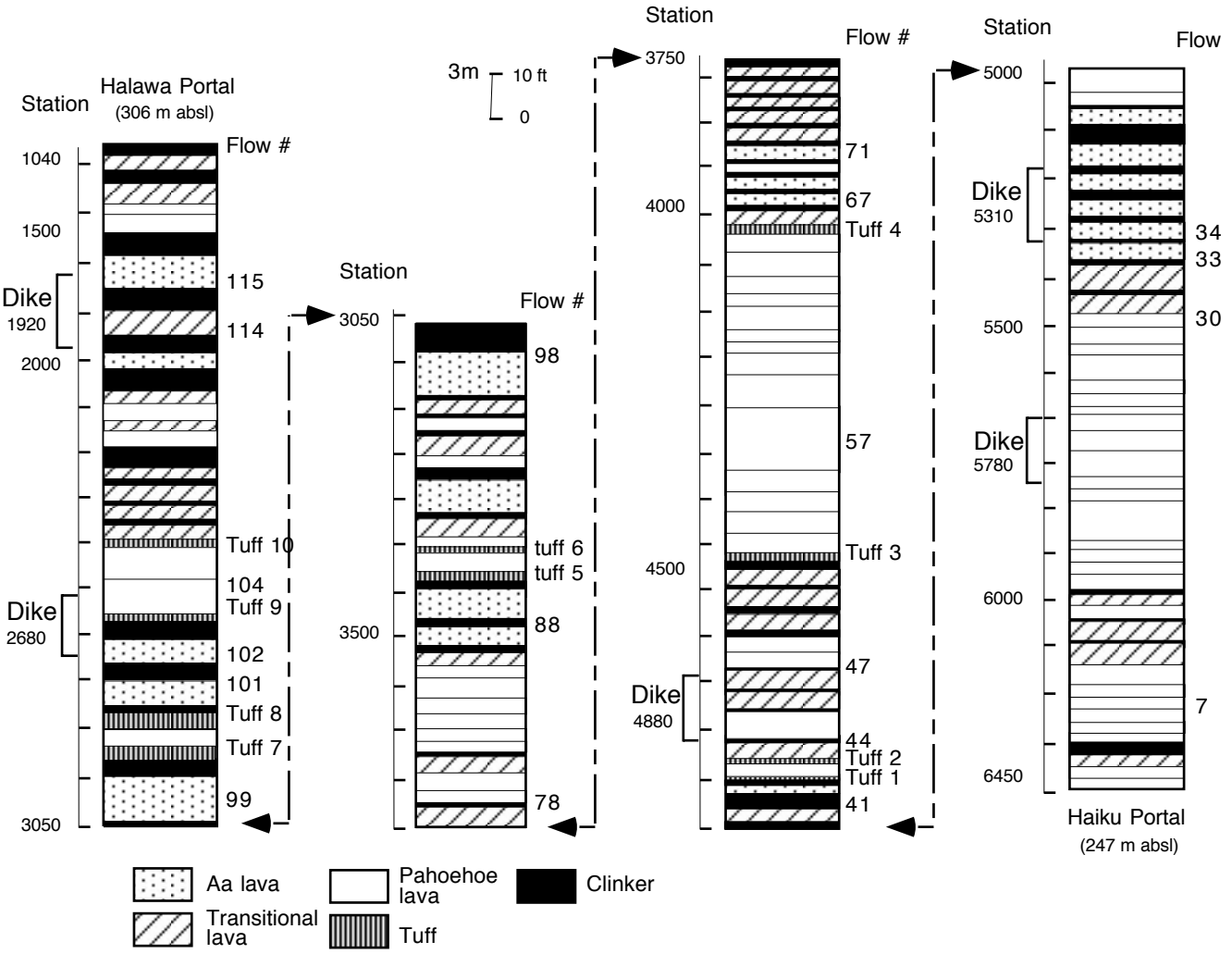

Fig. 3 Stratigraphic section showing flow types and location of tuffs and dikes in the main tunnel; *bracket* for each dike indicates flows cut by the dike. This is an inclined section spread out over the 1.6-km length of the tunnel, with the oldest flows exposed at the eastern Haiku portal. Flow numbers show the location of analyzed lava flows

well-developed post-shield alkalic stage. The younger Koolau Volcano, ~1.8–2.7 Ma (Doell and Dalrymple 1973), consists of a tholeiitic shield (Koolau Basalt) unconformably overlain by <1 Ma rejuvenated-stage lavas (Honolulu Volcanics). The Koolau shield is elongated parallel to the northwest rift zone which is clearly defined by abundant dikes on the highly eroded windward coast of Oahu (Fig. 1; Stearns and Vaksvik 1935; Wentworth and Winchell 1947). Studies of this dike complex have been important in establishing the structure of Hawaiian rift zones (Walker 1986, 1987). A shorter rift zone extends east–southeast from the caldera, and its subaerial termination is near Makapuu Head (Fig. 1).

Trans-Koolau exploratory tunnels

During construction of U.S. Interstate Highway H-3 through the Koolau Mountains, a nearly northeast-trending exploratory tunnel was excavated from North Halawa Valley on the western side of the Koolau Range to Haiku Valley on the eastern side (Fig. 1). The main tunnel has a diameter of 4.3 m and extends for 1652 m; from northeast to southwest the floor of the tunnel ascends from 247 to 306 m above sea level (Fig. 2). The portals and tunnels pass through the Koolau Basalt, the formation that forms the Koolau shield (Wentworth and Winchell 1947; Langenheim and Clague 1987). The 1.6-km tunnel exposes a stratigraphic section ~180 m thick, consisting of 119 lava flows and ten pyroclastic units, which is cut by five dikes (Fig. 3). In addition, at the western portal there are two tunnel branches that sample ~18 m of section (seven flows) above the main tunnel, thereby bringing the total thickness of continuous stratigraphy cut by the T–K tunnels to approximately 200 m. The main tunnel is sub-perpendicular to the northwest rift zone (Fig. 1) and cuts across the gently west-dipping (3–50) strata at an acute angle (Fig. 2).

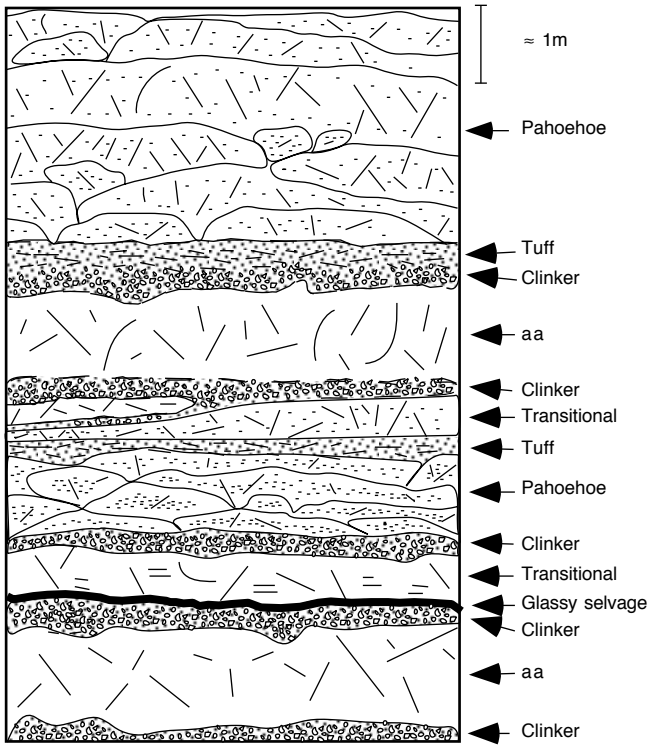

Fig. 4 Section showing typical physical features of the three flow types and the occurrence of clinker and tuff in the T–K tunnel

Wentworth and Winchell (1947; Fig. 2) and Wentworth (1951; Fig. 4) estimated the surface elevation of the Koolau shield at the end of shield building. Based on this estimate the T–K tunnel section, although now at a higher elevation, probably contains deeper and older shield lavas than the Makapuu section, a 250-m stratigraphic section of Koolau basalt exposed at Makapuu Head on the southeastern tip of Oahu (Fig. 1) that was studied by Frey et al. (1994) and Roden et al. (1994), i.e. presently there are ~400 m of lava flows overlying the central portion of the T–K tunnel (Fig. 2). By combining this overburden with estimates of erosion (Wentworth and Winchell 1947), we infer that the top of the tunnel section is approximately 500–600 m below the pre-erosional surface of the shield, whereas the top of the Makapuu section is within 50–100 m of the pre-erosional surface (Wentworth 1951).

An estimate of the minimum age of lava flows in the T–K tunnel section can be made from the K–Ar ages for lavas from Makapuu Head, 1.8±0.3 Ma [site B of Doell and Dalrymple (1973), four flows sampled from 30- to 223-m elevation] and Halawa Quarry, 1.9±0.1 Ma [site F of Doell and Dalrymple (1973), two flows sampled from 107- to 122-m elevation]. The Halawa Quarry site is estimated to be approximately 150 m below the pre-erosional surface of the Koolau shield (Wentworth and Winchell 1947; Wentworth 1951), and projection of the average dip of lava flows (4°W) from the centre of the T–K tunnel down North Halawa Valley shows that the top of the tunnel section is approximately 200–300 m below the Halawa Quarry site (Fig. 1). Therefore, the T–K tunnel section is older than 1.9 Ma; for a shield growth rate of 1 cm/year, the top of the T–K section is 40–50 ka older than the Makapuu section. However, because shield volcanoes build more rapidly near their summits than on their flanks (Lockwood and Lipman 1987, p. 513), it is possible that the T–K tunnel section, which is close to the caldera (Fig. 1), is only slightly older than the Makapuu section.

Sampling and methods

Geologic mapping of the exploratory tunnels was done at scales of 1:60 and 1:120 during tunnel construction in 1989. The collected samples are numbered according to their surveyed horizontal position (in feet) along the tunnel ranging from station 1040 at the top of the western Halawa portal to station 6457 at the bottom of the eastern Haiku portal; also the 126 identified lava flows are numbered sequentially beginning with the base of the lava sequence at Haiku portal (Fig. 3). Based on petrographic studies of 50 samples, 24 of the least altered samples from the main tunnel that include the range of petrographic types were selected for chemical analyses.

Major and trace element abundances were determined in duplicate by X-ray fluorescence (XRF) at the University of Massachusetts (Amherst). Precision and accuracy of the XRF data for Hawaiian tholeiitic basalts are typically better than 0.5% relative for major elements (except MnO, Na_2O, P_2O_5, which are 0.5–1%), and approximately 0.5–2% for trace elements (Rhodes 1996). Trace element abundances, including rare earth elements, were determined for a subset of seven samples by instrumental neutron activation analysis (INAA; Ila and Frey 1994). Abundances of FeO, H_2O^+, H_2O^- and CO_2 were determined by wet chemical methods at the Geological Survey, Pretoria, Republic of South Africa.

Petrography

The tunnel flows are aphyric to moderately porphyritic basalt, with <1%–16 vol.% total phenocrysts (>0.4 mm). Modal proportions of phenocrysts and microphenocrysts (0.05–0.4 mm) are shown in Table 1; more complete petrographic descriptions are in the Appendix. Olivine is the most abundant phenocryst phase in the relatively MgO-rich samples (e.g. 10.9% olivine in flow 30, sample 5483 with 11.9% MgO). Plagioclase and pyroxene are abundant in the more-evolved (MgO poor) lavas. The presence of orthopyroxene is a distinctive characteristic of Koolau lavas that reflects their high SiO_2 contents relative to other Hawaiian tholeiitic basalts. Orthopyroxene is more abundant than clinopyroxene as a phenocryst phase in most of these lavas (except samples 3143 and 6308); however, clinopyroxene is more abundant as microphenocrysts (except sample 5015). Plagioclase and Fe–Ti oxides are abundant as microphenocrysts in many lavas. Groundmass tex-

Table 1 Modal proportions of phenocrysts (Ph, >0.4 mm), microphenocrysts (Mph, 0.05–0.4 mm) and matrix in T–K tunnel samples. cpx clinopyroxene; opx orthopyroxene; plag plagioclase; oxide Fe–Ti oxides

Sample no.	Flow no.	Type[a]	Olivine		Cpx		Opx		Plag		Oxide	Matrix
			Ph	Mph	Ph	Mph	Ph	Mph	Ph	Mph	Mph	
6308	7	P	0.7	5.9	0.6	28.9	0.0	1.2	3.3	42.4	12.1	4.9
5483	30	P	10.9	0.7	0.0	11.2	0.6	0.5	1.3	11.8	0.7	62.0
5438A	33	A	0.1	0.3	0.0	22.1	0.6	0.0	0.0	19.0	0.6	57.3
5360	34	A	0.0	0.0	0.0	5.7	0.4	0.9	0.0	25.3	4.3	52.5
5015	41	T	3.8	1.5	0.0	2.1	2.3	3.7	1.1	5.8	5.9	73.8
4908	44	T	0.1	0.4	0.4	20.7	1.9	0.2	2.1	14.0	6.2	54.1
4784	47	T	0.0	0.9	0.0	11.1	0.0	2.7	0.8	22.3	10.6	51.6
4349	57	P	1.8	0.0	0.0	19.1	6.1	0.0	8.4	25.3	9.7	29.6
4026	67	T	0.0	2.3	0.0	3.9	1.4	0.0	1.7	6.6	9.2	74.9
3977	71	A	0.4	6.1	0.0	2.7	0.3	0.0	0.0	4.6	5.7	80.2
3754	78	P	0.0	1.2	0.0	0.0	0.0	0.0	0.0	8.7	16.7	73.4
3506	88	A	0.0	2.0	0.0	7.1	0.4	3.7	1.1	7.1	8.3	70.3
3143	98	A	0.7	0.2	0.4	33.9	0.1	1.1	0.6	40.5	15.2	7.3
3004	99	A	0.0	1.5	0.0	32.4	0.4	0.6	0.2	29.8	15.4	19.7
2819	101	A	0.4	0.2	0.1	10.9	0.7	1.4	0.1	24.4	10.0	51.8
2737	102	A	0.5	0.9	0.0	4.7	2.1	1.9	0.0	20.7	9.2	60.0
2394A	104	P	4.7	0.5	0.8	8.0	2.1	2.5	5.7	21.1	1.5	53.1
1808	114	T	0.0	0.7	0.3	4.3	0.6	3.9	1.2	25.7	17.3	46.0
1502	115	A	1.1	0.7	0.1	8.8	0.4	0.4	1.0	16.2	9.2	61.9
5800		D	1.9	0.3	0.0	12.7	3.1	2.9	1.3	23.1	40.9	13.8
5313		D	3.2	1.0	2.2	31.7	0.0	0.3	2.4	35.1	12.4	10.7
4886		D	0.0	0.2	0.2	35.5	0.6	1.3	0.2	41.9	15.8	6.3
2668		D	3.3	5.2	0.3	33.1	0.0	0.9	1.4	39.2	8.7	6.9
1929		D	0.0	1.2	0.2	20.7	1.2	21.2	0.3	41.8	6.1	7.3

[a]P, A, T and D designate pahoehoe, aa, transitional and dike, respectively

tures are generally fine-grained and holocrystalline, consisting of lath-shaped plagioclase with granular pyroxene and Fe–Ti oxides. Olivine phenocrysts are generally slightly to completely replaced by iddingsite, even in samples from the interior portions of the tunnel.

Flow morphology

Hawaiian lava flows are generally divided into two morphologic types (pahoehoe and aa), but some flows have characteristics transitional between these end members (Rowland and Walker 1987; Walker 1989). The distinctive characteristics of pahoehoe flows in the T–K tunnel are high vesicularity (20 vol.%) and the presence of glassy margins and tube structures, whereas the aa flows have lower vesicularity (<20%) and abundant clinker (Fig. 4). Transitional lava flows generally show some characteristics of both pahoehoe and aa.

Pahoehoe flows

Pahoehoe occurs both as thin, isolated flows and as thick compound flows (Fig. 4). In general, pahoehoe flows are highly vesicular, with 20–60 vol.% spherical vesicles ranging from less than 2 mm to approximately 1.5 cm in diameter. The upper and lower contacts are generally smooth and glassy. The pahoehoe tends to be more coarsely crystalline and often more porphyritic than do the aa and transitional flows. Three pahoehoe flows are highly porphyritic with 13–16% total phenocrysts and 25–54% microphenocrysts (flows 30, 57 and 104); only one pahoehoe flow is aphyric (flow 78; Table 1). A few lava tubes were identified within pahoehoe units; they are generally collapsed and filled with angular rubble or dense basalt.

Aa flows

The aa flows contain a dense crystalline core overlain, and in many cases underlain, by clinker that forms 30–60% of these flows (Fig. 4). The dense portion of aa flows generally has less than 20% vesicles, which are commonly deformed by shearing into elongate, irregular voids. In thin section, the aa flows are generally very fine grained and nearly aphyric, with less than 1% phenocrysts of olivine and/or orthopyroxene; clinopyroxene, plagioclase, and Fe–Ti oxide occur mainly as microphenocrysts, which are abundant in some aa flows (e.g. flows 98 and 99 in Table 1). Because of their lower vesicularity, the aa flows appear less altered than the pahoehoe flows.

Transitional flows

The transitional flows have characteristics intermediate between those of pahoehoe and aa. These flows generally have vesicle contents of 20–30%. The vesicles are subrounded to irregular in shape and variable in size. Circular voids, 9–60 cm in diameter, are common. They are similar to those in pahoehoe flows except that in the transitional flows they generally have smoother walls, which commonly are coated with frozen drips or stalactites of glassy lava. Clinker usually occurs at the top of transitional lava flows (Fig. 4), and in this way the upper parts of many transitional flows are more similar to aa than to pahoehoe. However, the basal portion of transitional flows can be highly vesicular with >30% vesicles (<5 mm) and a thin chilled margin of black glass at the lower contact (Fig. 4); thus, the base of transitional flows resembles that of pahoehoe more than that of aa. In general, flows mapped as transitional in the T–K tunnel have the characteristics of proximal aa; i.e. compared with distal aa flows, they are relatively thick with low vesicularity and a high proportion of clinker (Rowland and Walker 1987). Clinker breccia is a common constituent of transitional and aa lava flows. The thickness of clinker layers ranges from approximately 0.5–4.0 m and is generally proportional to the total thickness of the accompanying coherent transitional or aa flow.

Proportions of flow types and flow thickness

The ratio of pahoehoe to aa plus transitional flows is roughly 40:60 in the entire 200-m-thick tunnel section, but this ratio ranges from 50:50 in the east to 30:70 in the west (Table 2). The lower proportion of pahoehoe flows in the west may reflect a more distal environment of deposition, since it is further from the northwest rift zone. However, there are several factors that affect flow morphology, e.g. volatile content, temperature, eruption rate and slope angle. The discharge during eruption may be the single most important factor determining flow morphology (Pinkerton and Sparks 1976; Rowland 1987); thus, the relative proportions of the two flow types may not be simply related to distance from source vents.

In the T–K tunnel section average flow thicknesses increase from pahoehoe through transitional to aa lavas, and average thicknesses for each flow type are slightly greater in the west, i.e. in the upper part of the section (western half of tunnel), 50 lava flows total approximately 96 m in stratigraphic thickness for an average flow thickness of 1.9 m, whereas in the lower part of the section (eastern half of tunnel) the 76 flows average 1.3 m in thickness (Table 2). These relatively thin flows are consistent with a near-vent depositional setting. Proximal, near vent, Hawaiian lava flows are generally quite thin (<2 m), whereas distal flows are usually thicker (ca. 6 m; Macdonald 1967, pp 3–4). Specifically, for the Koolau shield, the 95 flows forming the near-rift axis section at Makapuu Head average 2.1 m in thickness, whereas Multhaup et al. (1989) showed that Koolau flows approximately 16 km west of the T–K tunnel range from 3 to 18 m in thickness.

Table 2 Mean lava flow thicknesses and relative volumes in the T–K tunnels (see Fig. 3)

Flow type	*N*	Total thickness (m)	Mean flow thickness (cm)	Volume (%)
Eastern (stratigraphically lower) main tunnel: Station 3750–6450				
Pahoehoe	46	50	108	51
Transitional	19	30	155	30
Aa	11	18	164	19
Total	76	97	128	
Western (stratigraphically higher) main tunnel: station 1040–3750 and tunnel branches at western portal				
Pahoehoe	21	26	121	27
Transitional	18	32	179	34
Aa	11	38	345	40
Total	50	96	191	

In summary, the physical characteristics of the T–K tunnel lavas, such as the east to west decrease in proportion of pahoehoe lavas and the low average flow thickness (<2 m), are consistent with these flows originating at vents on the nearby northwest rift zone. The southwest margin of the dike complex, which defines the boundary of the rift zone, is very close to the Haiku portal (Fig. 1).

Tuffs

Pyroclastic ash is a sporadic and minor constituent of Hawaiian volcanic eruptions (Decker and Christiansen 1984). The ten thin (0.3–1 m) interflow tuff beds in the T–K tunnel section probably represent pyroclastic eruptions, possibly from the Koolau caldera. These tuff beds occur in the central portion of the tunnel from stations 2300 to 5000 (Fig. 3). In addition, consolidated ash and reworked pyroclastic debris are a common component of the matrix in clinker layers at the top of aa and transitional flows (Fig. 4). Pyroclastic units in the T–K tunnel are vitric-crystal tuffs grading to lithic-vitric tuffs and lapilli tuffs in the terminology of Heiken and Wohletz (1985). Most beds grade upward from lithic-rich, poorly sorted, lapilli tuff to vitric-rich, well-sorted, fine-grained tuff. The upper part of most tuff beds is finely bedded (1–8 cm) to laminated (<1 cm); low-angle cross-lamination is present locally.

At Koolau Volcano ash deposits are expected to be most abundant in proximal settings downwind (southwest during tradewinds) of the caldera and rift zones. The numerous ash deposits in the T–K tunnel section are consistent with its location close to the caldera and southwest of the northwest rift zone, whereas ash layers are absent in the Makapuu Head section, which is not downwind from the caldera (Fig. 1).

Table 3 Major (weight percent) and trace (parts per million) element abundances determined by XRF for T–K tunnel loavas and dikes (flows are in order of stratigraphic height beginning with the bottom of the section). P, A and T denote lava morphology, i.e., pahoehoe, and aa transitional, Di denotes dikes (Fig. 2)

Flow no.	7	30	33	34	41	44	47	57	67	71	78	88	98	99	101	102	104	114	115	DIKE				
Sample no.	6308	5483	5438A	5360	5015	4908	4784	4349	4026	3977	3754	3506	3143	3004	2819	2737	2394A	1808	1502	5800	5313	4886	2668	1929
Flow type	P	P	A	A	T	T	T	P	T	A	P	A	A	A	A	A	P	T	A	Di	Di	Di	Di	Di
Stratigraphic height (m)	6	29	33	34	49	53	56	72	87	92	101	112	129	134	141	144	150	166	169	–	–	–	–	–
SiO_2	48.33	50.28	51.95	51.05	51.29	51.93	51.39	52.68	51.75	51.18	51.01	51.60	51.96	52.09	51.55	52.39	49.99	51.83	49.66	52.62	52.70	52.92	51.94	52.90
TiO_2	2.72	1.86	2.08	2.16	1.97	2.21	2.21	2.00	2.13	2.23	2.03	2.04	2.08	2.15	2.25	2.21	2.49	3.15	2.14	1.89	1.97	1.90	1.87	2.02
Al_2O_3	14.85	12.38	14.34	14.93	13.13	14.18	14.12	14.27	14.38	14.52	14.88	14.53	14.15	14.34	14.48	14.22	14.27	13.24	15.30	13.49	13.48	14.45	13.32	14.31
Fe_2O_3	3.88	0.59	1.03	1.84	0.79	1.48	1.90	0.00	0.52	1.13	3.70	2.97	4.40	3.43	3.26	3.33	5.62	4.11	4.93	3.05	2.22	0.17	3.18	2.11
FeO	8.34	9.89	9.20	8.84	9.84	9.04	8.74	9.79	9.88	9.24	7.30	7.57	6.24	7.08	7.30	7.03	6.04	8.24	6.61	7.24	8.26	9.63	7.52	7.88
MnO	0.17	0.16	0.15	0.16	0.16	0.16	0.16	0.15	0.16	0.16	0.16	0.16	0.15	0.16	0.16	0.15	0.17	0.17	0.16	0.15	0.15	0.15	0.16	0.15
MgO	7.00	11.92	6.69	6.90	9.42	6.44	7.04	7.18	6.59	6.88	7.15	7.08	7.06	6.77	7.24	7.05	7.07	5.26	7.02	8.03	7.76	7.03	8.72	7.30
CaO	10.92	8.96	9.98	10.36	9.40	10.03	10.34	9.54	10.16	10.23	10.37	10.03	9.86	10.02	9.78	9.55	10.43	9.12	10.32	9.21	9.32	9.85	9.50	9.52
Na_2O	2.43	2.15	2.36	2.50	2.21	2.43	2.31	2.67	2.41	2.44	2.44	2.55	2.51	2.46	2.61	2.64	2.29	2.77	2.45	2.46	2.48	2.57	2.23	2.79
K_2O	0.23	0.44	0.51	0.29	0.30	0.60	0.47	0.45	0.43	0.43	0.19	0.27	0.48	0.48	0.25	0.50	0.31	0.91	0.09	0.58	0.46	0.44	0.48	0.36
P_2O_5	0.34	0.22	0.24	0.23	0.23	0.27	0.26	0.24	0.25	0.27	0.21	0.24	0.26	0.27	0.30	0.30	0.30	0.43	0.24	0.24	0.25	0.25	0.24	0.27
H_2O^-	0.26	0.17	0.28	0.50	0.17	0.09	0.30	0.13	0.26	0.43	0.67	0.34	0.26	0.23	0.31	0.23	0.50	0.18	0.86	0.11	0.15	0.18	0.14	0.14
H_2O^+	0.66	0.45	0.58	0.70	0.29	0.61	0.55	0.11	0.47	0.62	0.66	0.45	0.43	0.41	0.42	0.47	0.64	0.62	0.80	0.38	0.17	0.43	0.47	0.26
CO_2	0.09	0.07	0.07	0.08	0.06	0.10	0.07	0.05	0.09	0.07	0.13	0.07	0.09	0.10	0.13	0.08	0.10	0.10	0.08	0.09	0.05	0.08	0.09	0.09
S	0.01	0.01	0.01	0. 01	0.01	0.01	0.01	0.01	0.01	0.01	0.01	0.01	0.01	0. 01	0.01	0.01	0.01	0.01	0.01	0.03	0.02	0.04	0.01	0.02
Total	100.23	99.55	99.46	100.54	99.27	99.58	99.87	99.27	99.49	99.84	100.91	99.90	99.93	100.00	100.04	100.16	100.23	100.14	100.67	99.58	99.44	100.09	99.88	100.12
Trace elements																								
Rb	2.4	4.9	5.7	3.3	3.1	6.3	5.1	6.2	4.6	4.5	2.0	2.7	5.0	5.4	2.6	6.3	3.4	11.3	0.5	6.6	6.4	5.4	5.9	4.5
Sr	492	337	371	379	332	406	394	352	376	401	349	374	385	394	437	428	417	433	387	381	404	410	374	430
Ba	175	77	84	76	69	107	98	98	77	86	70	72	89	97	119	109	90	157	71	95	106	92	88	110
Ga	23.0	18.1	19.7	20.8	19.1	19.4	20.4	19.7	20.9	19.5	20.1	19.7	19.9	20.7	20.7	21	20.4	22.1	19.3	19.6	19.4	19.5	18.8	20.4
Y	25.9	19.5	22.4	21.9	22.2	24.1	22.7	23.0	23.8	24.1	23.0	22.8	22.4	23.2	23.5	23.4	25.4	33.0	24.0	19.9	21.0	21.2	19.8	21.0
V	289	239	250	259	241	271	272	228	263	269	258	249	253	251	243	233	293	329	263	235	233	236	247	232
Cr	212	547	222	230	539	168	280	281	199	223	233	233	243	223	272	255	251	45	252	415	377	236	426	275
Ni	88	427	87	83	213	84	86	190	99	105	108	111	121	102	92	91	123	66	150	179	130	103	210	108
Zn	124	108	110	114	109	111	110	104	110	110	115	107	104	105	110	104	122	124	114	105	104	99	108	100
Zr	207	133	153	156	135	165	159	136	152	159	140	144	149	156	174	171	180	242	151	137	151	137	136	149
Nb	19.6	9.0	10.5	10.8	7.9	9.8	11.3	8.4	9.7	10.2	7.9	8.6	8.8	9.7	13.1	13.2	12.7	17.9	9.6	9.1	9.7	7.6	8.1	9.0
Ce	44	25	27	28	26	30	31	26	28	30	24	27	27	29	34	31	32	45	27	28	34	25	25	28

Table 4 Trace element abundances (parts per million) determined by instrumental neutron activation analysis

Flow no.	7	30	57	67	78	114	115
Sample no.	6308	5483	4349	4026	3754	1808	1502
Sc	28.4	23.9	25.1	27.8	27.9	27.5	28.7
Cr	226	539	291	192	216	43	248
Co	43.8	53.0	40.3	40.7	42.8	40.5	45.2
Hf	4.60	2.87	3.05	3.51	3.04	5.37	3.48
Ta	1.01	0.45	0.49	0.53	0.45	0.98	0.53
Th	1.06	0.51	0.75	0.52	0.46	0.96	0.64
La	16.7	8.81	9.70	10.2	8.35	17.8	10.1
Ce	42.7	23.5	25.7	27.6	23.8	46.8	25.3
Nd	28.2	16.0	16.9	20.9	17.6	30.9	19.3
Sm	6.77	4.23	4.70	5.16	4.70	7.75	5.11
Eu	2.21	1.47	1.62	1.81	1.64	2.49	1.79
Tb	1.02	0.63	0.82	0.85	0.73	1.15	0.89
Yb	1.94	1.48	1.89	1.85	1.78	2.43	1.87
Lu	0.28	0.23	0.29	0.28	0.27	0.35	0.28

Dikes

The T–K tunnels intersected five dikes (Figs. 2, 3); see Table 1 and Appendix for phenocryst mineralogy and petrography, respectively. Two dikes (1920 and 4880) are sparsely phyric and vesicular. Similar to most of the dikes in the northwest rift zone they strike northwest and dip steeply southwest. Two other dikes (2680 and 5310) strike northeast at high angles to the northwest rift zone and have columnar jointing perpendicular to dike margins. They lack vesicles and have 5–8% phenocrysts of olivine, clinopyroxene and plagioclase. Another dike (5780) is ~1 m thick, strikes N150 W, and dips 150–200 W away from the northwest Koolau rift zone. It has 1–3% phenocrysts of olivine, orthopyroxene and plagioclase.

Geochemical results

Geochemical studies of Koolau Basalt (Wentworth and Winchell 1947; Stille et al. 1983; Roden et al. 1984, 1994; Budahn and Schmitt 1985; Frey et al. 1994; Eiler et al. 1996; Lassiter and Hauri, in press) show that, relative to tholeiitic lavas from other well-studied Hawaiian shields, most Koolau lavas have: (a) higher SiO_2 and lower CaO and total iron contents at a given MgO content; (b) higher Al_2O_3/CaO and lower CaO/Na_2O; (c) high abundance ratios of Zr/Nb, La/Nb and Sr/Nb; (d) near bulk-earth $^{87}Sr/^{86}Sr$ and $^{143}Nd/^{144}Nd$ ratios, which define one end of the isotopic field displayed by Hawaiian shield lavas and contrasts with the relatively low $^{87}Sr/^{86}Sr$, and high $^{143}Nd/^{144}Nd$ of the younger, rejuvenated-stage Honolulu Volcanics; and (e) high $^{187}Os/^{188}Os$ and $\delta^{18}O$ relative to typical upper mantle. Because the tunnel flows erupted close to the caldera and are probably older than the well-studied flows from the Makapuu Head section on the southeast rift zone (Frey et al. 1994; Roden et al. 1994), geochemical data for the tunnel lavas (Tables 3, 4) are useful in defining the spatial and temporal compositional variations of Koolau shield lavas.

Effects of post-magmatic processes on lava compositions

The most altered lavas were not analyzed, but petrographic observations show that post-magmatic alteration occurred throughout the tunnel sections. The most extensive alteration is in saprolite zones at the portals. In general, within the main tunnel section the relatively porous pahoehoe flows are more altered than are the dense aa flows. However, both lava types have a similar range of total $H_2O + CO_2$ contents (0.29–2.58%) and Fe_2O_3/FeO ranges up to 0.93. In contrast, the dike samples are less altered (total $H_2O + CO_2$<0.70% and Fe_2O_3/FeO <0.42) (Table 3).

Previous studies of Hawaiian shield lavas from Koolau and younger volcanoes have shown that post-magmatic alteration results in preferential loss of K and especially Rb (Feigenson et al. 1983; Lipman et al. 1990; Frey et al. 1990, 1994; Chen et al. 1991). Consequently, altered shield lavas have K_2O/P_2O_5<1 and K/Rb >1000. The effects of such alteration are clearly shown by the T–K tunnel lavas, which define trends of decreasing K_2O/P_2O_5 and increasing K/Rb as H_2O content increases (Fig. 5A, B), and a wide range of K_2O content at a given MgO abundance (Fig. 6). The most altered analyzed lava in the tunnel section is sample 1502 (flow 115) from the top of the section (K_2O=0.09%, K_2O/P_2O_5=0.37, K/Rb=1490, Fe_2O_3/FeO=0.75, total volatiles=1.74%).

Abundances of other elements in Hawaiian shield lavas can also be affected by alteration (e.g. Lipman et al. 1990). Specifically for Koolau flows, many lavas with anomalously low K_2O/P_2O_5 have relatively low SiO_2 and high total iron contents (see Fig. 4 of Frey et al. 1994). Similarly, the T–K tunnel lavas with the lowest SiO_2 content, 6308 (flow 7) and 1502 (flow 115) from the bottom and top of the section, respectively (Fig. 3), have the lowest K_2O/P_2O_5 (Fig. 5C). The decrease in SiO_2 content of Koolau shield lavas caused by post-magmatic processes shows that the distinctively high SiO_2 content of unaltered Koolau lavas and glasses (Figs. 4 and 8 of Frey et al. 1994) is a primary feature of the Koolau basalt. In general, Koolau dikes are less altered and have high SiO_2 contents, >52% (Fig. 5 and Table 2c of Frey et al. 1994). The high SiO_2 contents of Koolau magmas have been attributed to melt segregation at relatively low pressure (Frey and Rhodes 1993; Frey et al. 1994), or a distinctive source component, eclogite, which is capable of yielding dacitic melt as a mixing component (Hauri 1996).

Major element compositions

Most of the analyzed lavas (19) and dikes (5) from the T–K tunnel define a range in composition that is similar to that of previously studied Koolau lavas (Fig. 6). Although the

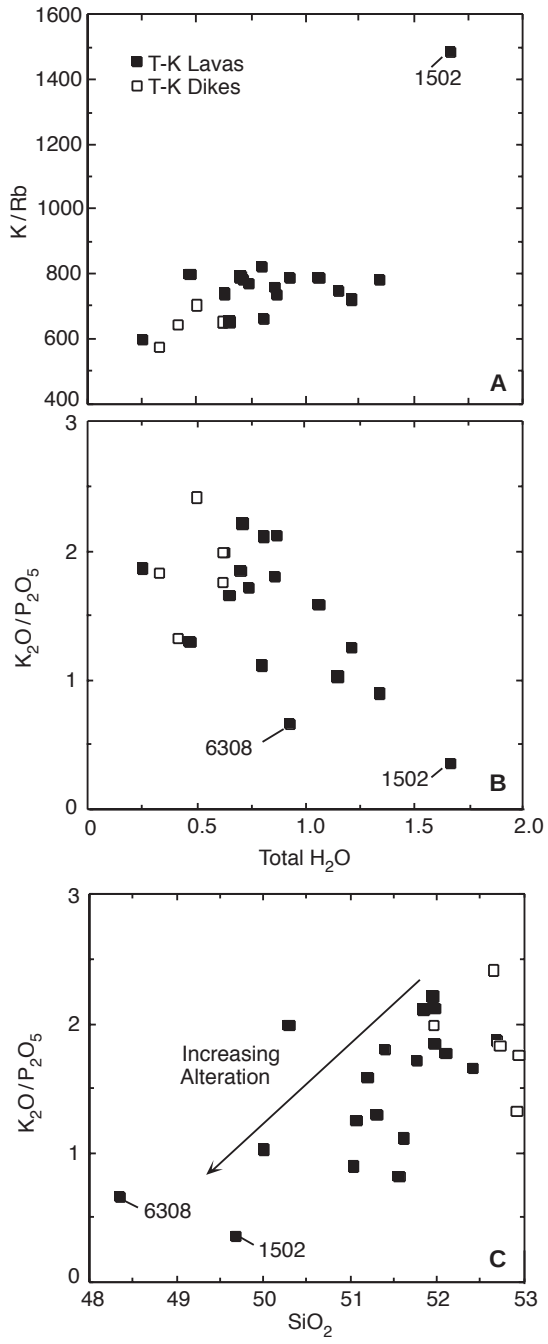

Fig. 5 A, B K_2O/P_2O_5 and K/Rb vs total water (H_2O) content (weight percent) for T–K tunnel samples showing that with increasing extent of post-magmatic alteration, i.e. increasing H_2O content, K_2O/P_2O_5 decreases and K/Rb increases. All of the dikes are relatively unaltered. **C** Shows that the most altered lavas (low K_2O/P_2O_5) also have lower SiO_2 (weight percent) contents (also see Fig. 4 of Frey et al. 1994). The two labelled samples, 1502 and 6308, have the lowest K_2O/P_2O_5 and SiO_2

tunnel and Makapuu Head lavas have a wide range in MgO content, primarily from ~5 to >16%, most flows, 16 of 19 in the tunnel section, have MgO=7.0±0.5%. This predominance of lavas with ~7% MgO is typical of other portions of the Koolau shield (Fig. 6) and the subaerial portions of other Hawaiian shields (e.g. Mauna Loa, Rhodes 1988; Kilauea, Garcia et al. 1996). Among the tunnel lavas, sample 5483 from flow 30, one of the oldest flows, is olivine rich (Table 1) and has the highest MgO content (11.9%; Fig. 6; Table 3). The oldest lava, sample 6308 (flow 7), has atypically low SiO_2 and high total iron contents (Fig. 6); coupled with low K_2O/P_2O_5; these characteristics may reflect post-magmatic alteration (Fig. 5). Sample 1808 from flow 114, one of the youngest lavas, is the most evolved, MgO=5.3%; relative to most Koolau lavas this sample has higher contents of total iron, TiO_2, K_2O, P_2O_5 and lower Al_2O_3 and CaO (Fig. 6). Only one previously analyzed Koolau basalt sample has a lower MgO content, i.e. sample WW11320, collected from Moanalua Valley only 1 km south of the T–K tunnel (Wentworth and Winchell 1947). It is unusual in having abundant, large plagioclase phenocrysts and very high Al_2O_3/CaO (2.06, Roden et al. 1984). Boulders of similar highly plagioclase-phyric basalt, possibly the same lava flow, were found near the Halawa portal of the T–K tunnel; therefore, this flow may be above the T–K tunnel.

Trace element abundances

Abundances of trace elements in lavas from the T–K tunnel section define trends very similar to those from other parts of the Koolau shield (Figs. 7–9). For example, Ni and Cr abundances are highly variable and positively correlated with MgO contents, whereas abundances of Zn (average of 111±6 ppm in the lavas) and V are much less variable and only weakly correlated with MgO content (Fig. 7). Abundances of Sc vary by only 7% (Table 4), and when the T–K tunnel lava compositions are adjusted to be in equilibrium with a common olivine composition, e.g. Fo_{88}, their Sc variation is further reduced to ~3%, i.e. an average of 23.7±0.7 ppm. For this calculation, the T–K tunnel whole-rock compositions were assumed to represent a crystallized melt, and equilibrium olivine, Fe/Mg K_D=0.3, was added in 1% increments to the lava composition until the calculated melt was in equilibrium with Fo_{88}; a Sc olivine/melt partition coefficient of 0.15 was assumed.

Abundances of Ba, Sr, Zr, Ce and Nb are positively correlated and vary by factors of 1.5–2.6 in the T–K samples, whereas Rb abundances, which were markedly affected by alteration, vary by a factor of ~22 and are not correlated with abundances of other incompatible elements (Fig. 8). An important result is the small variation in Y content (Fig. 8). In the 23 T–K tunnel samples with MgO>6.4% (i.e. omitting the most evolved sample 1808 from flow 114), Y varies only from 19.5 to 25.9 ppm. After these compositions are adjusted to be in equilibrium with a common olivine composition assuming a negligible Y content in olivine, the variation in Y content is further reduced; the mean Y content is 19.8±0.6 ppm for the 18 lavas and 18.2±0.3 ppm for the five dikes. A very similar result is found for 32 lavas with 6.5–12.4% MgO from Makapuu Head (Frey et al. 1994); after adjustment to be in equilibrium with a common olivine composition, the mean Y abundance is 20±1 ppm. Similarly, eight dikes from the caldera complex with

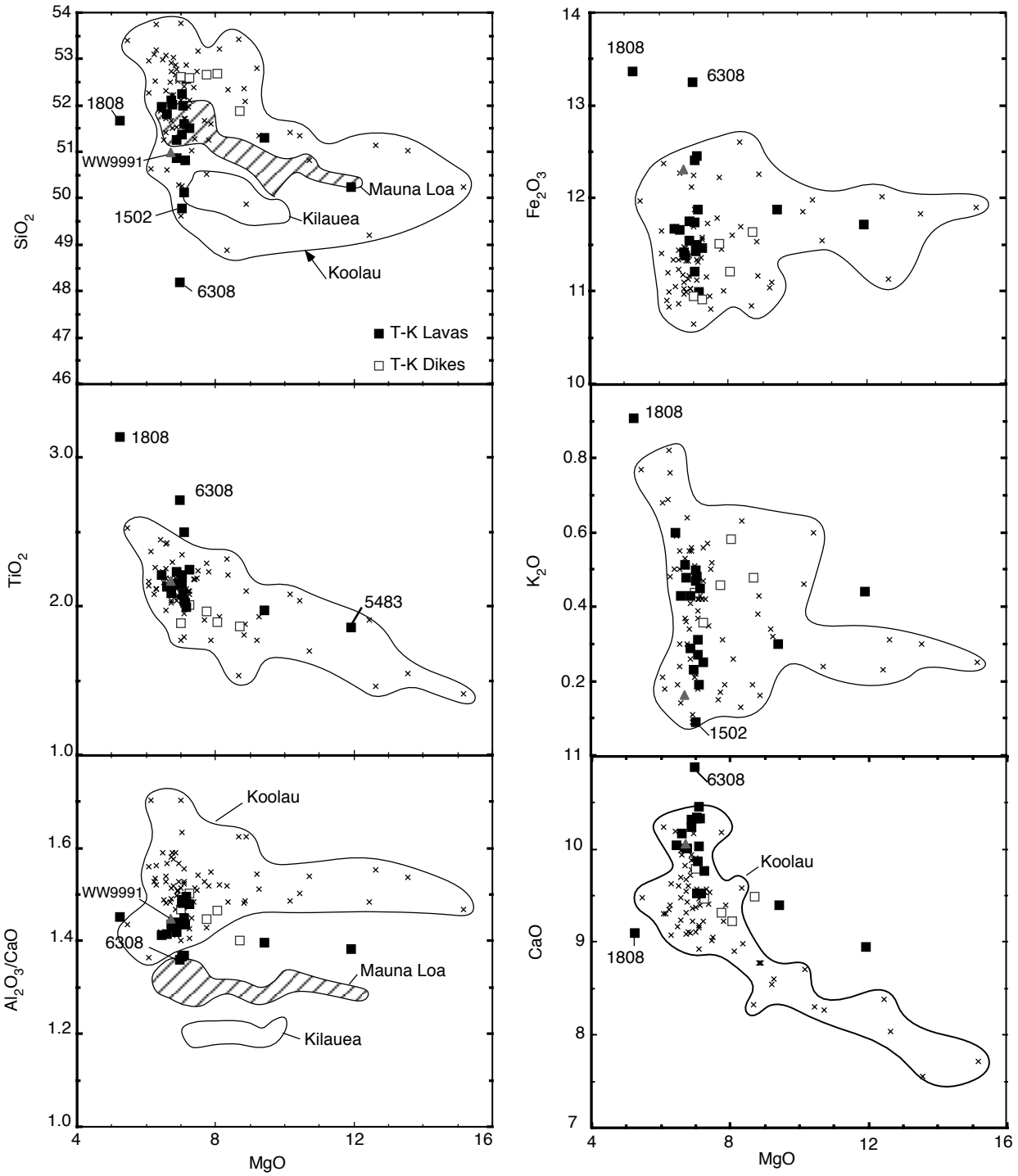

Fig. 6 Abundances of SiO_2, Fe_2O_3 (total iron), TiO_2, K_2O and CaO, (all in weight percent) and Al_2O_3/CaO vs MgO content (weight percent). Field encloses data (*x*) for 72 Koolau samples with <16% MgO (Frey et al. 1994). In general, the T–K tunnel samples lie within the field for these samples. However, T–K sample 6308 is distinct with relatively low SiO_2 and high Fe_2O_3 and CaO. Also, the T–K sample with the lowest MgO content (sample 1808) is relatively enriched in Fe_2O_3, TiO_2 and K_2O, and is depleted in CaO. Also shown (*triangle* in SiO_2 and Al_2O_3/CaO panels) is isotopically distinct Koolau lava WW9991 (Roden et al. 1984). The relatively high SiO_2 and Al_2O_3/CaO that is typical of Koolau lavas is shown by comparison with fields for historic Mauna Loa lavas (Rhodes and Hart 1995) and recent Kilauea lavas (Puu Oo episodes 12–53; Garcia et al. 1996)

6.1–8.1% MgO have a mean Y content of 18.4±0.8 ppm when adjusted to the same olivine composition (data from Frey et al. 1994). In both lava suites, T–K tunnel and Makapuu Head, this constancy in Y content is accompanied by more than a factor of two variation in Nb abundance (and abundances of other highly incompatible, relatively immobile elements), even after adjustment of the lavas to be in equilibrium with a common olivine composition.

Similar to the uniformity of Y abundance in Koolau lavas, Yb abundance in five T–K tunnel lavas with 6.6–11.9% MgO (Table 4) were derived from parental mag-

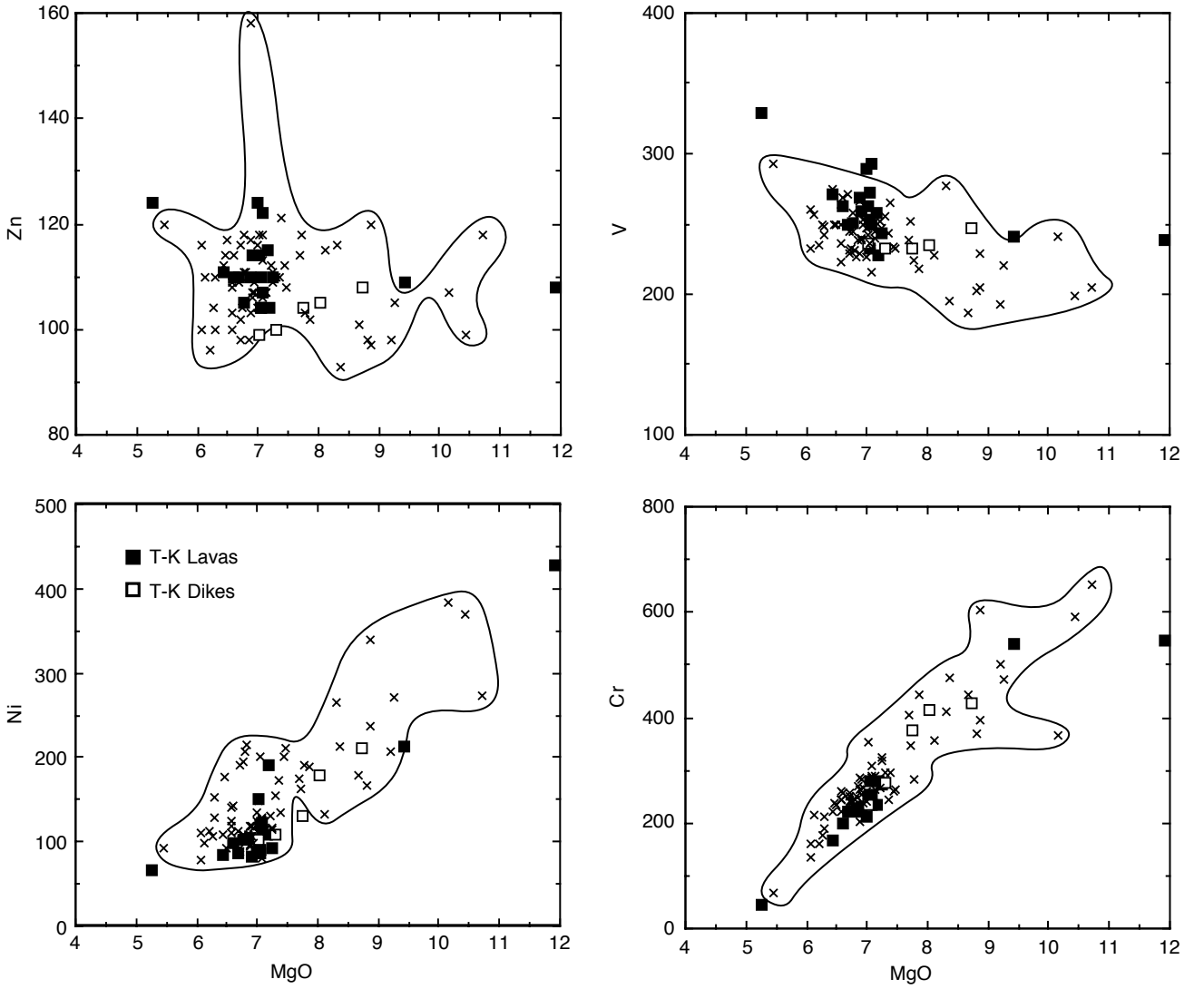

Fig. 7 Abundances of Ni, Cr, Zn and V (all in parts per million) vs MgO content (weight percent) in T–K tunnel samples. In general, the T–K samples plot within the field for 72 Koolau samples studied by Frey et al. (1994)

mas with very similar Yb contents, i.e. a mean of 1.55±0.06 ppm after the lava compositions are adjusted to be in equilibrium with Fo_{88} olivine. This Yb abundance is very similar to that inferred for Makapuu Head lavas, i.e. when the 20 Makapuu Head lavas with 6.5–12.4% MgO are adjusted to be in equilibrium with Fo_{88} olivine, the mean Yb content of the parental magmas is 1.50±0.15 ppm.

Six of the seven T–K tunnel samples analyzed for rare earth elements (REE) have chondrite-normalized REE patterns similar to those for the majority of lavas from Makapuu Head (Fig. 9). One T–K tunnel sample, 6308 from the lowermost flow studied, is distinguished by higher abundances of light REE (LREE); similarly, a single flow, KOO 30, from the Makapuu Head section is anomalously rich in LREE (cf. Fig. 7 of Frey et al. 1994). The relative enrichment of sample 6308 in LREE is consistent with its low Zr/Nb (Fig. 10). Although sample 6308 has low K_2O/P_2O_5 (Fig. 4B), indicative of post-magmatic alteration, the relatively high La/Yb and low Zr/Nb are probably magmatic features. Except for sample 6308, all of the T–K tunnel samples have relatively high Zr/Nb, >12 (Fig. 10), characteristic of Koolau lavas (see Fig. 5 of Roden et al. 1994).

Petrogenesis

Shallow level processes

Sixteen of the 19 T–K tunnel lavas have MgO contents within the narrow interval of 6.4–7.2% (Fig. 11). A dominance of lavas with ~7% MgO is also found in the Makapuu Head Section where 30 of 39 lavas have 6.4–7.8% MgO (Frey et al. 1994). Most historic Mauna Loa lavas also have MgO in this range (see Fig. 2 of Frey and Rhodes 1993). Rhodes (1988) proposed that this near uniformity in MgO content results from a long-lived steady-state magma reservoir in which frequent input of magma with olivine as the liquidus phase maintains (buffers) the reservoir magma at

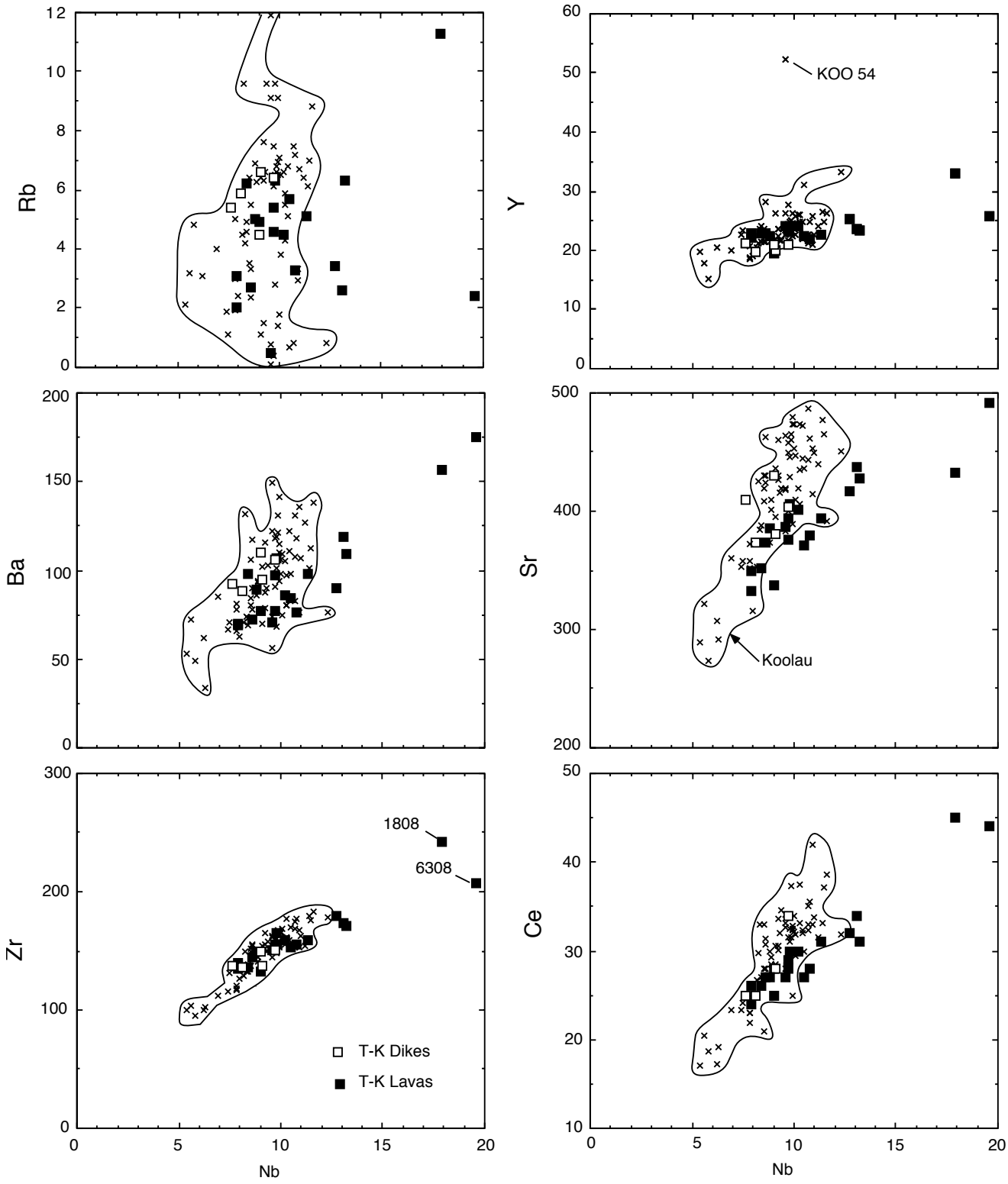

Fig. 8 Abundances of Zr, Ce, Ba, Sr, Rb and Y vs Nb content (all in parts per million) in T–K tunnel samples. Except for Rb, whose abundance was markedly affected by post-magmatic alteration, abundances of these elements in Koolau lavas vary by about a factor of two and are positively correlated. Y abundances are the least variable; sample KOO 54 has very high Y because of late-stage weathering (see Frey et al. 1994). In general, the T–K samples plot within the field for 72 Koolau samples studied by Frey et al. (1994), but two tunnel samples, 1808 and 6308, have significantly higher Nb contents. The high Nb content of sample 1808 reflects its evolved composition (5.26% MgO; see Fig. 6), but sample 6308 was derived from a geochemically distinct parental magma

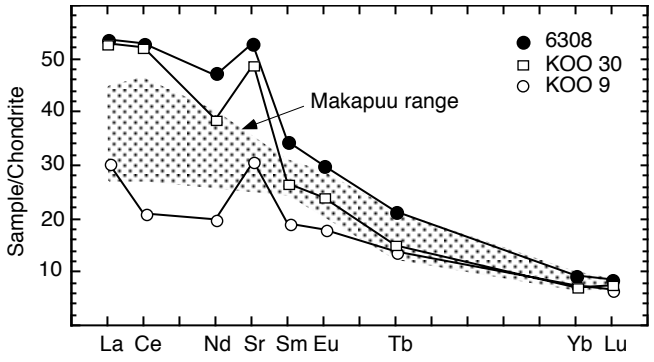

Fig. 9 Chondrite-normalized REE plot for Koolau lavas. The *stippled field* indicates the range for 20 Koolau lavas from Makapuu Head (Frey et al. 1994) and includes six of the seven T–K lavas analyzed for REE. The geochemical end members in the Makapuu Head section are samples KOO 9 and KOO 30; sample 6308, the geochemically anomalous T–K lava, has a REE abundance pattern similar to that of KOO 30. For these three samples, Sr is plotted next to Nd (using a chondritic value of 15.6 for Sr/Nd). Each of these samples has Sr/Nd greater than that of chondritic or primitive mantle, but KOO 9, with the lowest REE content, has the highest Sr/Nd (24.1)

the four phase reaction point: olivine+melt=pigeonite+clinopyroxene+plagioclase. The reservoir magma can evolve to highly differentiated magmas with <6% MgO only when magma supply is very low. Although periods of relatively low magma supply occur in rift zones (e.g. Wright and Fiske 1971; Yang et al. 1997), the T–K lavas, which erupted from the northwest rift close to the caldera, have compositions that reflect control by frequent supply of olivine-saturated magma.

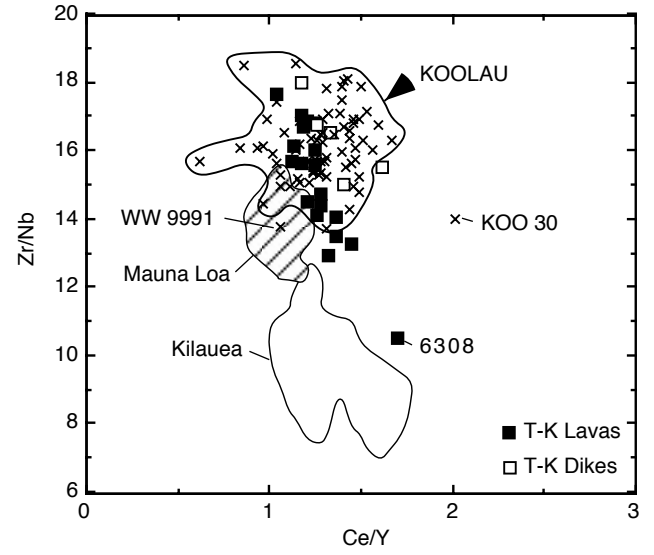

Fig. 10 Zr/Nb vs Ce/Y showing that Kilauea and Mauna Loa lavas are largely distinct in Zr/Nb, and that Koolau samples (both T–K tunnel, previous data *x* of Frey et al. 1994, and isotopically anomalous Koolau lava WW9991 from Roden et al. 1984), overlap in Zr/Nb with Mauna Loa lavas. In detail, the field for Koolau samples extends to higher Ce/Y than the field for Mauna Loa lavas. Also, T–K lava sample 6308 is anomalous and has Zr/Nb similar to that of Kilauea lavas. Data sources are: this paper, Roden et al. (1984) and Frey et al. (1994) for Koolau; Rhodes and Hart (1995) for Mauna Loa field; Chen et al. (1996) and Garcia et al. (1996) for Kilauea field

The T–K tunnel lavas analyzed do not define systematic temporal compositional trends (Fig. 11), but realistic evaluation of temporal compositional trends requires analysis of all flows in the section. However, most of the T–K tunnel lavas have the distinctive geochemical features of Koolau lavas, such as high Al_2O_3/CaO, Zr/Nb and Sr/Nb (Fig. 11). The most evolved lava, sample 1808, with only 5.28% MgO is an exception. Relative to most Koolau lavas, it has slightly lower Zr/Nb and much lower Sr/Nb (Fig. 11). The compositional characteristics of this sample, relatively low MgO, CaO and Al_2O_3 and high abundances of incompatible elements (Figs. 6, 8), reflect extensive fractionation of plagioclase and clinopyroxene. The compatible nature of Sr in the fractionating plagioclase led to the anomalously low Sr/Nb ratio. In contrast, sample 6308 from the oldest flow has a typical MgO content (7.0%), but it has distinctly lower Sr/Nb and Zr/Nb than other Koolau lavas (Fig. 11). We infer a geochemically distinct primary magma for this sample.

Constraints on source composition: correlations between isotopic and incompatible element abundance ratios

The isotopic differences between various Hawaiian shields establish that geochemically distinct sources contribute to their growth (e.g. Staudigel et al. 1984; Stille et al. 1986; West et al. 1987; Roden et al. 1994; Lassiter and Hauri, in press). There are also systematic compositional differences between Hawaiian shields that may be related to differences between sources and/or differences in processes, such as variations in mean extent of melting or the mean pressure of melt segregation (Frey and Rhodes 1993; Frey et al. 1994; Hauri 1996). Differences in source composition should result in correlations between compositional features and isotopic ratios.

There has been considerable discussion of intershield differences in isotopic ratios and composition (e.g. Frey and Rhodes 1993; Roden et al. 1994; Hauri 1996; Lassiter and Hauri, in press) but there has been relatively little evaluation of correlations between composition and isotopic ratios of lavas within an individual shield. The largest intrashield variability in $^{87}Sr/^{86}Sr$ and $^{143}Nd/^{144}Nd$ occurs in the Koolau, Kahoolawe and Lanai shields (West et al. 1987; Roden et al. 1994; Basu and Faggart 1995; Fig. 12, this paper). Among these shields, Koolau is the most thoroughly studied; therefore, Koolau lavas are useful in evaluating intrashield correlations between isotopic and compositional variations.

Except for flow 7 (sample 6308) at the bottom of the section, all of the T–K tunnel lavas have the relatively high Zr/Nb characteristic of Koolau lavas (Fig. 10; Frey and Rhodes 1993; Frey et al. 1994). Although Zr/Nb can be affected by variations in extent of melting, Zr/Nb and isotopic ratios are correlated in Hawaiian shields, with Koolau and Kahoolawe shield lavas extending to the highest Zr/Nb and $^{87}Sr/^{86}Sr$ (Fig. 5 of Roden et al. 1994). Hence distinctive Zr/Nb ratios (as well as Sr/Nb and La/Nb; Roden et al. 1994) are interpreted as source characteristics. In order to

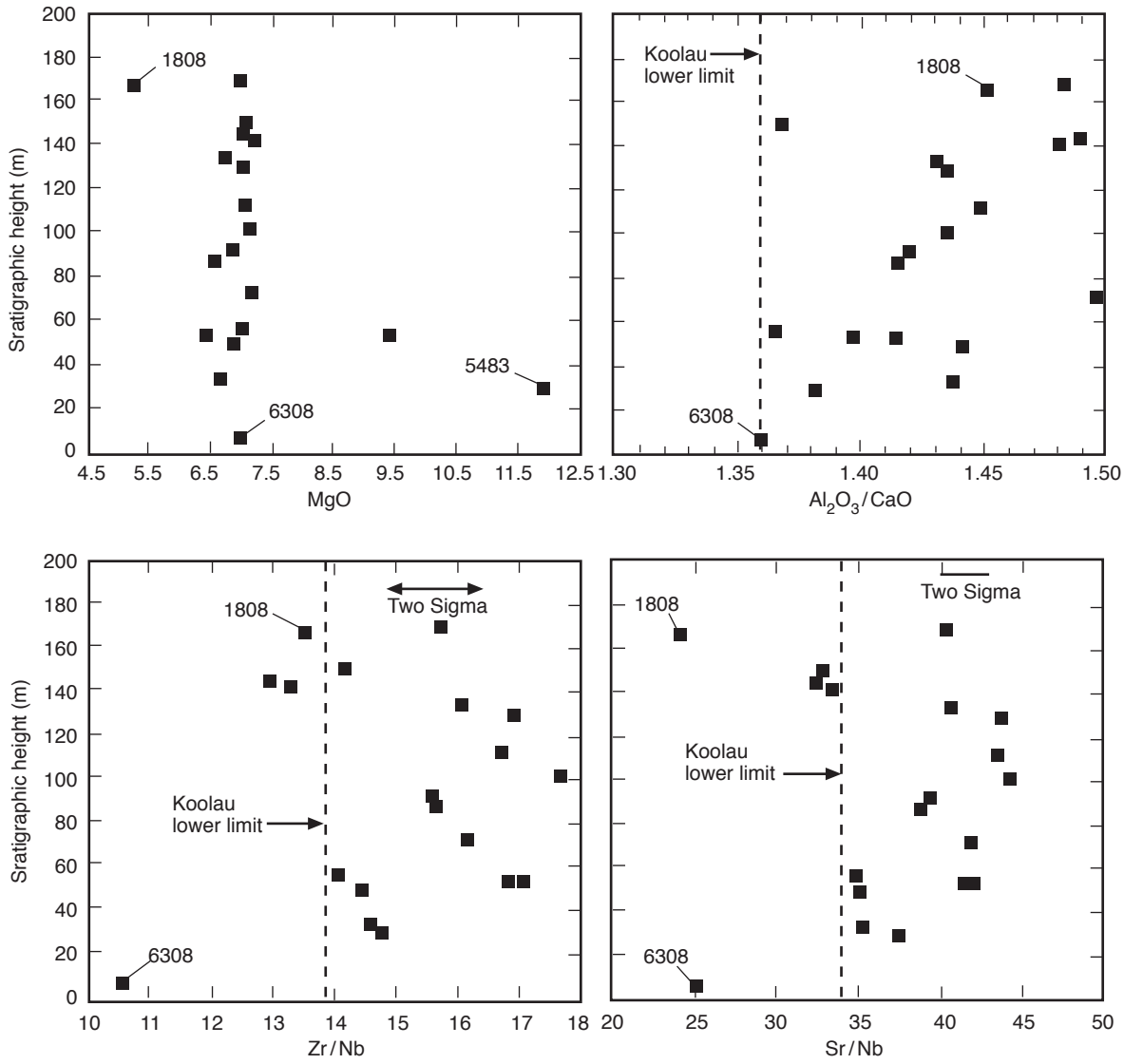

Fig. 11 MgO (weight percent), Zr/Nb, Al_2O_3/CaO and Sr/Nb vs stratigraphic height in metres in the composite T–K tunnel section. Relatively high values for these ratios distinguish Koolau shield lavas from other Hawaiian shield lavas. The *dashed lines* indicate the lower limits for Koolau lavas studied by Frey et al. (1994). Most of the T–K tunnel lavas have these distinctive high ratios, but two T–K samples, 1808 and 6308, have significantly lower Sr/Nb and 6308 also has lower Zr/Nb. Note that Sr/Nb (and La/Nb; see Fig. 11 of Frey et al. 1994) in many Koolau lavas exceeds that of primitive mantle and MORB (29.6 and 38.6, respectively)

determine if the atypically low Zr/Nb of sample 6308 is accompanied by atypical isotopic ratios, this sample was analyzed for Sr and Nd isotopic ratios. Sample 6308 has $^{87}Sr/^{86}Sr$=0.703568±10 and $^{143}Nd/^{144}Nd$=0.512981±10 (analyses done at MIT; La Jolla standard=0.511850 and NBS-987=0.710240 for $^{143}Nd/^{144}Nd$ and $^{87}Sr/^{86}Sr$, respectively). These ratios for sample 6308 are within the field for Kilauea lavas (Fig. 12) and further extend the isotopic range of Koolau lavas. A Kilauea-like isotopic component is also found in some relatively old, perhaps >130 ka, submarine lavas from Mauna Loa (Gurriet et al. 1988; Kurz et al. 1995; Rhodes et al. 1997), and it may be a component present in all Hawaiian shields. In contrast, the high $^{87}Sr/^{86}Sr$/low $^{143}Nd/^{144}Nd$ component is known to occur only in the ~2 Ma Koolau shield and in two, Lanai and Kahoolawe, of the six volcanoes forming the slightly younger Maui volcanic complex (Fig. 12; West et al. 1987; Basu and Faggart 1995).

Sample 6308 has Zr/Nb (10.6), Sr/Nb (25.1) and La/Nb (0.85) ratios that are well outside the field of other Koolau lavas (Figs. 10, 11) and as with Sr and Nd isotopic ratios, these abundance ratios overlap with those of Kilauea lavas (e.g. Fig. 10, this paper, and Fig. 5 of Roden et al. 1994). A previously analyzed Koolau lava (sample WW9991; Roden et al. 1984) has Sr and Nd isotopic ratios within the field for Mauna Loa lavas (Fig. 12). Relative to sample 6308, sample WW9991 has higher Zr/Nb (13.8), Sr/Nb (36.2) and La/Nb (1.15), which overlap with the Mauna Loa field (Fig. 10; Fig. 5 of Roden et al. 1994); therefore, as concluded previously (Frey and Rhodes 1993; Roden et al. 1994), these incompatible element abundance ratios are correlated with isotopic ratios; hence, they are inferred to be a source

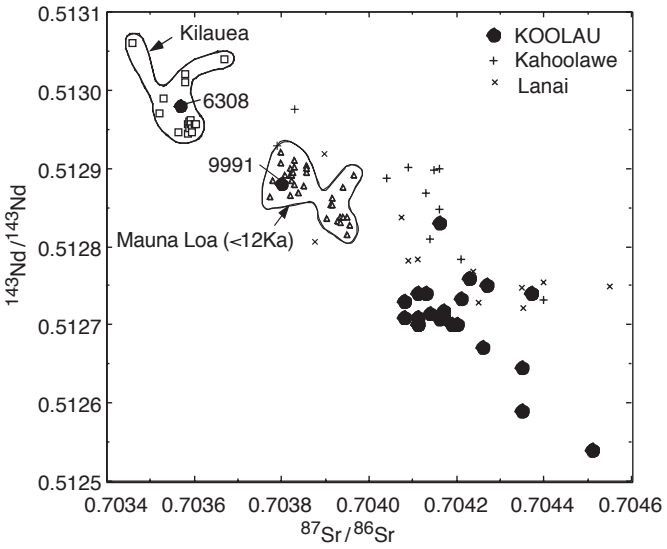

Fig. 12 $^{143}Nd/^{144}Nd$ vs $^{87}Sr/^{86}Sr$ for shield lavas from Kilauea, Mauna Loa, Koolau, Lanai and Kahoolawe volcanoes. The fields for Kilauea and Mauna Loa are distinct, whereas those from Koolau, Lanai and Kahoolawe are heterogeneous and extend to lower Nd and higher Sr isotopic ratios. Koolau tunnel sample 6308 overlaps with the Kilauea field, and Koolau sample WW 9991 overlaps with the Mauna Loa field. Data sources: Kilauea (Hofmann et al. 1984; Garcia et al. 1996); <12,000 years Mauna Loa (Kurz et al. 1995; Rhodes and Hart 1995); Lanai (West et al. 1987; Basu and Faggart 1995); Kahoolawe (Leeman et al. 1994) and Koolau (this paper; Roden et al. 1984, 1994; Bennett et al. 1996; Lassiter and Hauri, in press)

characteristic. Certainly, ratios such as Zr/Nb are changed by the partial melting process, but the effects of variable extents of melting do not obliterate the significant differences between source components.

Constraints on source composition: correlations between isotopic ratios and major element composition

Relatively high SiO_2 content and Al_2O_3/CaO are distinctive characteristics of Koolau basalt. All of the T–K tunnel lavas have higher Al_2O_3/CaO (1.36–1.50) than do lavas forming the Kilauea and Mauna Loa shields (Fig. 6, this paper, and Fig. 11 of Frey et al. 1994). Such high Al_2O_3/CaO is not a result of post-magmatic alteration or low-pressure processes, e.g. the evolved flow 114 (sample 1808) with 5.26% MgO retains the high Al_2O_3/CaO of more MgO-rich lavas (Fig. 11). We conclude that high Al_2O_3/CaO is a characteristic of primary Koolau magmas; however, it is likely that Al_2O_3/CaO reflects variable extents of partial melting and the relative roles of residual clinopyroxene and garnet, rather than a source characteristic (Frey et al. 1994; Kinzler 1997).

Two alternatives have been proposed to explain relatively high SiO_2 abundances. Relative to other Hawaiian shields, Mauna Loa and Koolau shield lavas have high SiO_2 contents (Hauri 1996), but unlike Koolau lavas, Mauna Loa lavas do not range to the extreme Sr, Nd and Pb isotopic ratios (e.g. Fig. 12). Moreover, lavas from the Koolau and Kahoolawe shields range to similarly high $^{87}Sr/^{86}Sr$ (Fig. 12), but Kahoolawe lavas do not have relatively high SiO_2 contents (Hauri 1996). On this basis, Frey and Rhodes (1993) concluded that high SiO_2 abundance was not inherited from the source but was caused by melt segregation at relatively low pressure. Hauri (1996) noted that the high SiO_2 contents of Koolau lavas require melt segregation at depths of 30–45 km, which are less than the lithospheric thickness beneath the island of Hawaii. However, decompressional melting of the plume to shallower depths during formation of the Koolau shield may have been facilitated by the proximity to the Molokai fracture zone (Basu and Faggart 1995; Wessel 1993).

Hauri (1996) proposed that the incoherence between SiO_2 abundance and isotopic ratios described by Frey and Rhodes (1993) could be explained if the intershield correlation between the average SiO_2 content and average isotopic ratio (Nd and Os) is hyperbolic. If such a correlation is valid, then high SiO_2 content is likely to be a source feature. Pursuing this interpretation, Hauri (1996) concluded that Koolau Basalt contains ~14% of a dacitic melt derived by partial melting of a mantle source containing at least 5% quartz-bearing garnet pyroxenite. The geochemical characteristics of Lanai shield lavas were not considered by Hauri (1996). They are, however, similar to Koolau lavas in that Lanai lavas also range to >0.7044 in $^{87}Sr/^{86}Sr$ (Fig. 12), and Lanai lavas with $K_2O/P_2O_5>1$ typically have high SiO_2 contents (52–53% at ~7% MgO; West et al. 1992). Therefore, following the interpretation of Hauri (1996), lavas from the Koolau and Lanai shields contain a dacitic melt component, but tholeiitic lavas from other shields, such as Loihi and Haleakala with relatively low SiO_2 contents, contain little if any of this dacitic component.

While there is no doubt about the relatively high SiO_2 content of primary Koolau lavas, there are weaknesses in the argument used to conclude that variations in major element compositions and isotopic ratios are correlated. Firstly, Kahoolawe Volcano, another shield with lavas ranging to >0.7044 in $^{87}Sr/^{86}Sr$ (Fig. 12), is not characterized by high SiO_2 contents. The averages for the Kahoolawe shield are consistent with the hyperbolic SiO_2 vs $^{143}Nd/^{144}Nd$ trend emphasized by Hauri (1996), but they are not consistent if $^{87}Sr/^{86}Sr$ is used rather than $^{143}Nd/^{144}Nd$. This inconsistency results because at a given $^{87}Sr/^{86}Sr$, Kahoolawe lavas are offset from the Koolau field to higher $^{143}Nd/^{144}Nd$ (Fig. 12). This offset could be caused by post-magmatic increases in $^{87}Sr/^{86}Sr$, but three Kahoolawe lavas which range widely in $^{87}Sr/^{86}Sr$ were acid-leached prior to isotopic analyses (West et al. 1987). Secondly, Mauna Loa lavas are isotopically distinct from the Koolau (Fig. 12) but have high SiO_2 contents similar to Koolau lavas (see Fig. 1a, c of Hauri 1996, but note that the Koolau average of Hauri is biased to low SiO_2 content because it includes lavas that lost SiO_2 during post-magmatic alteration). Moreover, significant isotopic variations in relatively old Mauna Loa lavas are not correlated with variations in SiO_2 content (Gurriet et al. 1988; Rhodes et al. 1997).

Given the isotopic heterogeneity of Koolau lavas, a better test of compositional-isotopic correlations than comparing shield averages is to evaluate within-shield correlations.

Koolau samples 6308 (this paper) and WW9991 (Roden et al. 1984) have Sr and Nd isotopic ratios such as those of Kilauea and Mauna Loa lavas, respectively (Fig. 12). Do these two Koolau lavas have distinctive major element compositions? Certainly, sample 6308 has major element characteristics unlike those of other Koolau lavas, e.g. it has a low SiO_2 content and low Al_2O_3/CaO (Fig. 6). These results support the hypothesis of correlated major element and isotopic variations in Hawaiian shield lavas. A caveat, however, is that sample 6308 is altered (K_2O/P_2O_5 ~0.65; Fig. 5); therefore, it is possible that the low SiO_2 content is not a magmatic feature. However, the absence of orthopyroxene phenocrysts in sample 6308 (Table 1) is consistent with a low SiO_2 magma. Sample WW9991, which has Sr and Nd isotopic ratios similar to those of Mauna Loa lavas (Fig. 12), is not as distinctive in major element composition; however, the differences in major element composition between the Koolau and Mauna Loa shield lavas are small relative to those between Koolau and Kilauea shield lavas (Fig. 6).

Constraints on source mineralogy

We suggest another test of the hypothesis of Hauri (1996) that Koolau lavas contain a dacitic melt component derived from partial melting of garnet pyroxenite. If we assume that the relative proportion of dacitic component reflects the proportion of garnet pyroxenite in the source, then high SiO_2 shield lavas should show the effects of equilibrating with larger amounts of residual garnet, i.e. they should have lower abundances of Sc, Y and HREE, elements that are compatible in garnet during partial melting (Green 1994). Therefore, we compare abundances of Sc, Y and Yb in lavas from Koolau, Mauna Loa and Kilauea volcanoes. We choose to compare these volcanoes because the two active volcanoes, Kilauea and Mauna Loa, are geochemically distinct, with Mauna Loa lavas having relatively high SiO_2 content (Frey and Rhodes 1993; Hauri 1996). Most importantly, data sets for these three volcanoes have in large part been obtained by using the same analytical facilities, XRF at University of Massachusetts and INAA at the Massachusetts Institute of Technology, thereby eliminating problems arising from analytical bias between laboratories. A nontrivial problem in comparing the geochemical characteristics of primary magmas at different shields is assessing the effects of post-melting processes, such as fractional crystallization, magma mixing and post-magmatic alteration. Because olivine is the dominant phenocryst in most shield lavas, olivine fractionation and/or addition have been commonly used to infer primary magma compositions that have either a common MgO content or that are in equilibrium with a common olivine composition (e.g. Hofmann et al. 1984; Hauri 1996). Frey and Rhodes (1993) suggested that

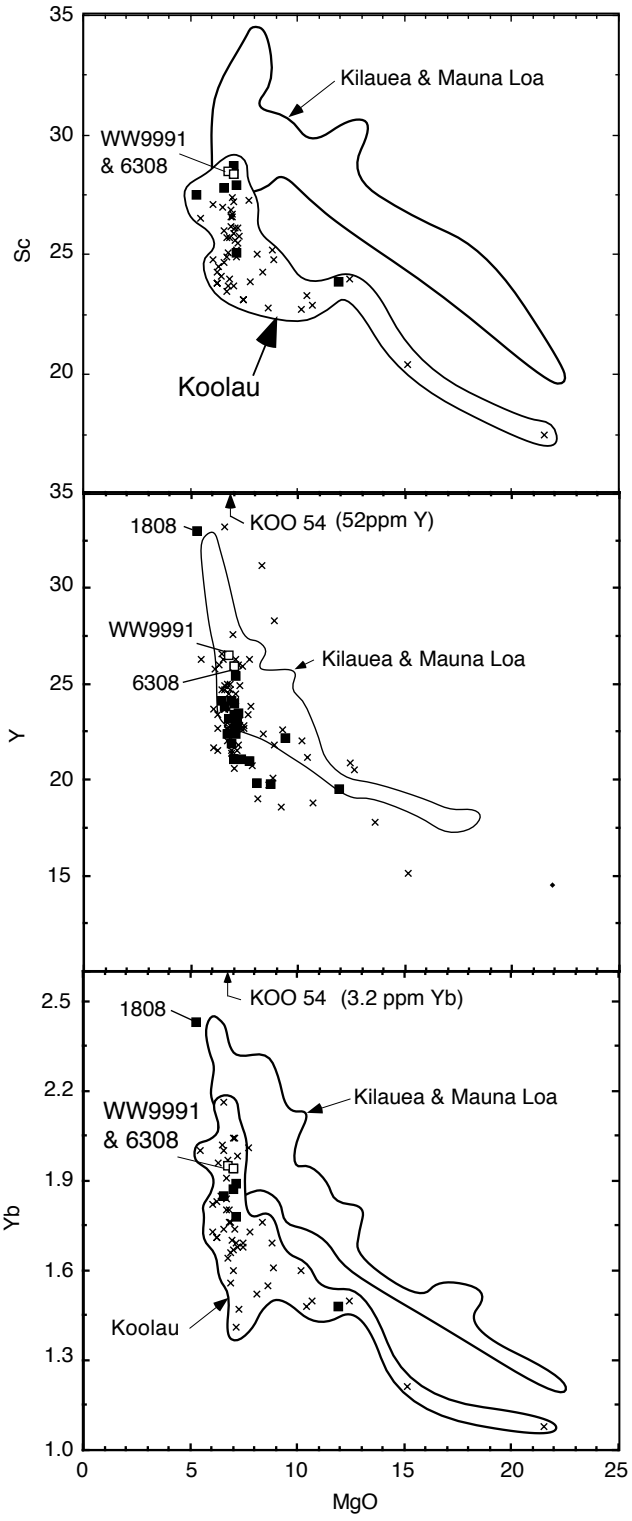

Fig. 13 Sc, Y and Yb (all in parts per million) vs MgO content (weight percent) in lavas from Koolau, Kilauea and Mauna Loa volcanoes. Although there is scatter, especially in Koolau lavas with ~7% MgO, it is clear that the mean trend for Koolau lavas has lower Y, Sc and Yb abundances, at a given MgO content, than the trends for Kilauea and Mauna Loa lavas. These intershield differences are obvious despite the complexity caused by rare examples of Y and REE enrichment caused by post-magmatic alteration of Koolau lavas, such as KOO 54 (see Frey et al. 1994). In contrast, the isotopically anomalous Koolau lavas, 6308 and WW9991 (*open squares*) plot within the field for Kilauea and Mauna Loa lavas. Data sources: Koolau (this paper, and Frey et al. 1994); Mauna Loa (Rhodes and Hart 1995); Kilauea (Hofmann et al. 1984; Chen et al. 1996; Garcia et al. 1996)

when sufficient data are available, a better approach is to use MgO variation plots, because no assumptions are made about post-melting processes.

The Sc-MgO trend (Fig. 13) shows clearly that at a given MgO content, Koolau lavas have lower Sc contents than do Kilauea and Mauna Loa lavas, a fact that was recognized by Budahn and Schmitt (1985) and Frey et al. (1994). Since Sc is compatible in clinopyroxene and garnet relative to a basaltic melt (Green 1994), a larger proportion of residual clinopyroxene and garnet is inferred for Koolau lavas.

Because Y and Yb are compatible in garnet relative to melt and clinopyroxene (Green 1994; Harte and Kirkley 1997), these elements can distinguish the relative roles of residual garnet and clinopyroxene. The Y-MgO trend shows that at a given MgO content, Y abundance is generally lower in Koolau lavas than in Kilauea and Mauna Loa lavas, but there is large scatter in the Koolau data (Fig. 13). This scatter results in part from a post-magmatic weathering process that locally redistributes Y, REE and P into groundmass phosphate (Frey et al. 1994, p. 1449). The same complexity affects Yb abundances in Koolau lavas, but there is no doubt that, on average, Koolau lavas define a lower Yb-MgO trend than do Kilauea and Mauna Loa lavas (Fig. 13). In summary, the relatively lower Sc, Y and Yb abundances in Koolau lavas are consistent with a larger proportion of residual garnet during generation of Koolau lavas (also see Norman and Garcia 1997).

The two Koolau lavas with relatively low $^{87}Sr/^{86}Sr$ and high $^{143}Nd/^{144}Nd$ are an exception to this generalization. Samples 6308 and WW9991 have higher abundances of Y, Yb and Sc than do most Koolau lavas (Fig. 13). In particular, Sc abundances are among the highest found in Koolau lavas. Abundances of Y and Yb in these two samples are not as high as in low MgO, highly evolved lavas, such as sample 1808, and even higher abundances occur in lavas with post-magmatic phosphate, e.g. KOO 54 (Frey et al. 1994). Nevertheless, the relatively high Y, Yb and Sc contents of the two lavas with the lowest $^{87}Sr/^{86}Sr$ and highest $^{143}Nd/^{144}Nd$ show that the garnet-rich component is characterized by relatively high $^{87}Sr/^{86}Sr$ and low $^{143}Nd/^{144}Nd$.

In summary, our tests of the proposal that relatively high SiO_2 contents reflect a component derived by partial melting of garnet pyroxenite (Hauri 1996) are largely consistent with this hypothesis. Compared with other Hawaiian shield lavas, Koolau lavas with relatively high $^{87}Sr/^{86}Sr$ and low $^{143}Nd/^{144}Nd$ have relatively low abundances of Sc, Y and Yb, elements controlled by residual garnet. In contrast, an anomalous Koolau lava (T–K tunnel sample 6308) with relatively low $^{87}Sr/^{86}Sr$ and high $^{143}Nd/^{144}Nd$ has higher abundances of Sc, Y and Yb and a relatively low SiO_2 content, although it is uncertain whether the low SiO_2 content is a magmatic or alteration feature.

Origin of the Koolau source

The inferred high-MgO primary magmas and the forsteritic-rich olivines in Koolau and other Hawaiian shield lavas require a dominantly peridotite source (e.g. Clague et al. 1995; Norman and Garcia, in press). Koolau shield lavas have the Sr, Nd and Pb isotopic characteristics associated with the EM 1 mantle component (Hart 1988). Commonly, these isotopic characteristics have been interpreted as reflecting a non-peridotite source component, i.e. recycled oceanic crust including a small proportion of ancient pelagic sediment (e.g. Weaver 1991; Chauvel et al. 1992). For Koolau lavas this interpretation is strongly supported by their relatively high $^{18}O/^{16}O$ and $^{187}Os/^{188}Os$ and low $^{206}Pb/^{204}Pb$ ratios (e.g. Lassiter and Hauri, in press). The relative enrichment of Sr (e.g. high Sr/Nd abundance ratios) in melt inclusions trapped in olivine phenocrysts of Mauna Loa lavas has been used to argue that the protolith of the recycled igneous crust was dominantly plagioclase-rich cumulate gabbro (Sobolev et al. 1998). This inference is also valid for Koolau lavas. Frey et al. (1994) found that Koolau lavas range in Sr/Nd from the primitive mantle value of 15.6–24, a factor of 1.5. Norman and Garcia (1997, in press) also found that relative to picrites from other Hawaiian shields, Koolau picrites have higher Sr/Nd. Fig. 9a of Frey et al. (1994) shows that the highest Sr/Nd ratios are in lavas with the lowest incompatible element content (also see Hofmann 1998). This trend is seen in Fig. 9 (this paper), where the largest Sr anomaly is in relatively depleted sample KOO 9, whereas the Kilauea-like Koolau lava, 6308, has a relatively small Sr anomaly.

The strongest evidence for recycled ancient sediment in the Koolau source is the low $^{206}Pb/^{204}Pb$ of Koolau lavas, which define one extreme of the inverse $^{87}Sr/^{86}Sr$–$^{206}Pb/^{204}Pb$ trend defined by all Hawaiian shield lavas (e.g. Roden et al. 1994; Lassiter and Hauri, in press). The inverse trend of X/Nb (where X=Zr, La or Sr) vs $^{206}Pb/^{204}Pb$, whose extreme is also defined by Koolau lavas (e.g. Fig. 14 of Yang et al. 1994) indicates that recycled sediment is the source of the high X/Nb ratios. Indeed, recent pelagic sediments are relatively depleted in Nb, and this relative depletion may not be obliterated during dehydration in subduction zones (e.g. Fig. 4 of Weaver 1991). In particular, Sr/Nb and La/Nb ratios in Koolau lavas range to values higher than those of primitive mantle and average MORB (Fig. 11 and Table 4 of Roden et al. 1994). Such values are most readily explained by a recycled sedimentary component. Also in modern pelagic sediments, such as red clays, high La/Nb is associated with low U/Pb (Plank and Langmuir, 1998). With aging, the low U/Pb leads to relatively low $^{206}Pb/^{204}Pb$. Consequently, ancient pelagic sediment with such characteristics can explain the inverse correlation between X/Nb and $^{206}Pb/^{204}Pb$ that is defined by Hawaiian shield lavas (e.g. Fig. 14 of Yang et al. 1994). Other incompatible element abundance ratios in Koolau lavas are also consistent with this scenario. For example, the anomalously low Rb/Sr of unaltered Koolau lavas (Roden et al. 1994) is consistent with relative loss of Rb from the oceanic plate during dehydration in a subduction zone.

Finally, Koolau lavas have modestly high $^{3}He/^{4}He$ (11–14 times the atmospheric ratio), and Roden et al. (1994) noted that crustal recycling does not account for the relatively high $^{3}He/^{4}He$ typical of Hawaiian shield lavas. A similar paradox, i.e. high $^{3}He/^{4}He$ associated with heavy

isotopic ratios that reflect recycled oceanic crust, occurs in Samoan lavas (Farley 1995). Apparently, the high $^{3}He/^{4}He$ signature is associated with the peridotitic component.

Summary

A 200-m-thick section of the Koolau shield, 126 basaltic lava flows with ten thin interflow tuffaceous units, is exposed in the 1.6-km-long Trans-Koolau (TK) tunnel. This tunnel is close to the northwest rift zone of the Koolau shield. The lavas dip gently southwest. With increasing distance from the rift zone, the proportion of pahoehoe to aa flows decreases and mean flow thickness increases. These trends and the presence of tuffs and dikes in the tunnel section are consistent with derivation of the flows from vents along Koolau`s northwest rift zone. Compared with previously studied Koolau shield lava flows, this tunnel section formed closer to the caldera, and the lowermost flows are inferred to be older.

The majority, 16 of the 19 analyzed tunnel flows, have similar MgO contents, 6.8±0.4%. This limited range is also characteristic of previously studied Koolau lavas and other Hawaiian shields, such as Mauna Loa. Rhodes (1988) suggested that this buffering reflects operation of a steady-state magma reservoir in which magma replenishment is sufficient to maintain the reservoir magma at the olivine+melt=pyroxene+plagioclase reaction point.

Compared with other Hawaiian shield lavas, Koolau lavas and dikes of varying age from diverse parts of the shield have distinctive geochemical features, such as relatively high SiO_2, Al_2O_3/CaO, Sr/Nd, Zr/Nb, La/Nb, $^{87}Sr/^{86}Sr$, $^{187}Os/^{188}Os$ and $^{18}O/^{16}O$ coupled with low $^{143}Nd/^{144}Nd$ and $^{206}Pb/^{204}Pb$, which define the extremes for Hawaiian shield lavas. These isotopic characteristics have been interpreted to reflect a source component that is recycled oceanic crust containing a small proportion of ancient pelagic sediment (e.g. Fig. 7 of Chauvel et al. 1992; Lassiter and Hauri, in press). Relative to other Hawaiian shields, such as Kilauea and Mauna Loa, the source of Koolau lavas contained a larger proportion of recycled oceanic crust. Several geochemical features of Koolau lavas reflect the igneous portion of this recycled crust:

1. The lower abundances of Sc, Y and heavy REE at a given MgO content reflect the control of residual garnet created by metamorphism of the igneous crust to garnet pyroxenite.
2. The high Sr/Nd indicates abundant cumulus plagioclase in the oceanic crust prior to metamorphism.
3. The high $^{187}Os/^{188}Os$ reflects aging of the high Re/Os crust.

Other geochemical characteristics of Koolau lavas reflect the role of recycled sediment:

1. The relatively low $^{206}Pb/^{204}Pb$ reflects aging of low U/Pb sediments.
2. The Nb depletion, as manifested by La/Nb greater than primitive mantle and MORB, is characteristic of pelagic clays.

Although most Koolau lavas have relatively high $^{87}Sr/^{86}Sr$ (~0.7040–0.7042) and low $^{143}Nd/^{144}Nd$ (~0.51270–0.51275), the lowermost flow in the tunnel section extends the isotopic range of Koolau lavas to much lower $^{87}Sr/^{86}Sr$ (0.703568) and higher $^{143}Nd/^{144}Nd$ (0.512981). These ratios overlap with those of lavas from Kilauea Volcano. This sample is also compositionally different from other Koolau lavas, thereby providing additional evidence for coupled variations between lava composition and isotopic ratios (Roden et al. 1994; Hauri 1996). The presence of a lava with Kilauea-like geochemical characteristics at the bottom of the tunnel section is similar to recent results showing that Kilauea-like geochemical characteristics occur in older Mauna Loa lavas (e.g. Rhodes et al. 1997). This lowermost flow in the T–K tunnel section establishes a positive correlation between X/Nb (X=Zr, La or Sr) and $^{87}Sr/^{86}Sr$ for Koolau shield lavas that is analogous to that defined by all Hawaiian shields (Roden et al. 1994). This correlation shows that a varying proportion of recycled oceanic crust in the source was also important during growth of the Koolau shield.

Acknowledgements Field work for this project was done by M.J. and R.W. while employed by Parsons Brinckerhoff-Hirota Associates (PBHA) of Honolulu, Hawaii, with able assistance from D.C. Rose, A.P. Matulac and R.A. Hagen. P.B.H.A. is thanked for allowing the authors to pursue the more academic aspects of this study during their employment and for financing most of the analytical work. Much of the paper was compiled and written while the first author was a Research Associate with the Economic Geology Research Unit of the University of the Witwatersrand, Johannesburg, South Africa. Within 3 months of receiving journal reviews (June 1994), Michael C. Jackson was very seriously injured in an automobile accident. To date, he is slowly recovering but he is not yet capable of preparing a revised manuscript. In tribute to Mikeís dedication to this research effort and the importance of Koolau Volcano to understanding Hawaiian volcanism, F.F. and M.G. prepared this revised version using reviewer comments, recent literature and newly acquired geochemical data. We thank D. Coleman (Sr and Nd isotopic analyses of flow 7) and P. Ila (neutron activation) for obtaining these new data. A. Saal provided important help in figure preparation. Discussions with D. Francis and G.P.L. Walker were very helpful. We thank C.Y. Chen, E. Hauri, J.M. Rhodes, M. Roden and an anonymous reviewer for their comments, and the editor, W. Hildreth, for his patience. This is SOEST contribution number 4720.

Appendix: Petrographic descriptions of T–K tunnel samples

Sample	Flow	Rock type	Description
6308	7	Pahoehoe	Slightly weathered, moderately vesicular (10–20% irregular vesicles, 2–10 mm in diameter). Porphyritic with ol, plag and cpx phenocrysts and glomerocrysts and opx microphenocrysts. Olivine is altered to iddingsite. Fe–Ti oxides are abundant; secondary Mn-oxide coats veiscles and occurs as dendrites in the matrix
5483	30	Pahoehoe	Highly vesicular, porphyritic with fine-grained holocrystalline matrix. Olivine phenocrysts (5%) up to 2.5 mm and subhedral, rare cpx phenocrysts (<0.5 mm) and opx phenocrysts (<1 mm). Some olivine has iddingsite alteration (0.1 mm on rim)
5438A	33	Transitional	Slightly vesicular and aphyric with vesicle trains defining flow lamination. Some large voids, up to 1 mm. Very fine-grained, with opx phenocrysts (up to 0.4 mm) and oliv phenocrysts (up to 0.5 mm) and rare olivine microphenocrysts
5360	34	Aa	Slightly vesicular (<5% irregular vesicles, 1–10 mm), very fine-grained and nearly aphyric. Less than 1% plag and cpx phenocrysts and glomerocrysts, few opx phenocrysts. Holocryst alline matrix with abundant Fe–Ti oxides
5015	41	Transitional	Slightly vesicular and porphyritic with subhedral ol phenocrysts, (elongated crystals up to 3 mm), subhedral opx phenocrysts and few plag microphenocrysts. Holocrystalline fine-grained matrix with abundant oxides
4908	44	Transitional	Slightly vesicular (5–10%) and porphyritic with opx, plag and cpx phenocrysts (0.1–1.0 mm) and plag microphenocrysts
4784	47	Transitional	Slightly vesicular with rare plag phenocrysts (anhedral, 0.2 mm, resorbed and pitted). Rare opx microphenocrysts (0.1 mm)
4349	57	Pahoehoe	Pahoehoe porphyritic with anhedral olivine phenocrysts (up to 2 mm), subhedral plag pheno crysts (0.5–2 mm) and anhedral opx phenocrysts (1 mm)
4026	67	Transitional	Very fine grained with rare opx microphenocrysts (0.1–0.3 mm), plagioclase laths, interstitial (0.05 mm) cpx and abundant 0.01–0.03 mm oxides
3977	71	Aa	Slightly vesicular with 1% olivine phenocrysts, rare 0.2 mm opx phenocrysts, interstitial 0.05 mm cpx and a holocrystalline matrix with abundant secondary oxides
3754	78	Pahoehoe	Highly vesicular (30–40%), and very fine-grained with abundant oxides, rare plagioclase microlites and altered (iddingsite)-oliv microphenocrysts
3506	88	Aa	Slightly vesicular (<5%), irregular-shaped vesicles which are stretched parallel to flow lami nation. Medium-grained porphyritic with<1% phenocrysts of opx (often with cpx rims), plag and euhedral oxides in a holocrystalline groundmass
3143	98	Aa	Fresh and fine-grained plag, cpx and oxides in a matrix with little glass, moderately vesicular with euhedral oliv (up to 2 mm) and abundant plag microphenocrysts (<0.5 mm), abundant oxides (0.025–0.05 mm), opx microphenocrysts (0.01–0.1 mm) and cpx microphenocrysts (<0.01 mm)
3004	99	Aa	Fresh, fine-grained gray matrix with 10% vesicles (elongate and irregular). A matrix of mostly cpx (0.1–0.5 mm), and oxides (0.01–0.2 mm) with larger plag microphenocrysts, rare opx phenocrysts (up to 1 mm), one glomerocryst of intergrown plag and cpx
2819	101	Aa	Slightly weathered and fine grained. Opx phenocrysts and rare olivine phenocrysts with iddingsite rims. Matrix of plag and cpx
2737	102	Transitional	Fine-grained with 10% vesicles (some round, some stretched). Holocrystalline with abundant oxides (primary?), opx microphenocrysts (0.05–0.10 mm) and opx phenocrysts often resorbed, oliv phenocrysts (to 0.7 mm) with iddingsite rims, groundmass of plag and cpx
2394A	104	Pahoehoe	Highly weathered with black-orange-brown banded flow margin. Plag, opx, cpx and olivine (some iddingsite) phenocrysts in a felty, devitrified glass matrix
1808	114	Transitional	Slightly weathered with 5–10% vesicles (irregular shape). Plag, opx and cpx phenocrysts, and rare microphenocrysts

Sample	Flow	Rock type	Description
1502	115	Aa	Moderately weathered and medium gray with 5% deformed vesicles with black vesicle linings. A felty groundmass (30–40% microlaths) with abundant oxide crystals (15%). A few glomerocrysts of olivine (iddingsite) and plag. Relatively unweathered olivine (1 mm) and two large cpx (1–2 mm)
5800		Dike	Slightly vesicular and medium-grained intersertal texture. Olivine and plag phenocrysts, opx phenocrysts (1–2 mm), and abundant secondary oxides filling matrix interstices, but olivine is mostly unaltered. Opx phenocrysts with cpx rims
5313		Dike	Non-vesicular and holocrystalline. Very fine-grained, equigranular-intersertal, plag and cpx intergrowths with rare olivine phenocrysts (<0.5 mm)
4886		Dike	Moderately vesicular and porphyritic. Opx phenocrysts with cpx rims, fine-grained holocrystalline matrix, abundant secondary oxides, isotopic, high-relief vesicle-filling mineral (zeolite–heulandite?), and pockets of very dark groundmass with disseminated oxides
2668		Dike	Fresh, non-vesicular and fine-grained, matrix of plag, olivine and cpx, and dark glass (<10%). Plag (1 mm), feathery olivine (0.05–0.5 mm) often in clots of 0.5-mm grains, some with opx rims, plag is subhedral and skeletal, very fine oxides in matrix and olivine+rare opx microphenocrysts
1929		Dike	Centre of dike is lightly weathered with large evenly distributed vesicles. Patches of partially altered divitrified glass, rare olivine microphenocrysts (altered to iddingsite), feathery plag laths and euhedral opx needles (up to 1 mm), subhedral cpx (0.05–0.1 mm)

References

Basu AR, Faggart BE (1995) Temporal isotopic variations in the Hawaiian mantle plume: the Lanai anomaly, the Molokai fracture zone and a seawater-altered lithospheric component in Hawaiian volcanism. Am Geophys Union Geophys Monogr 95: 149–159

Bennett VC, Esat TM, Norman MD (1996) Two mantle-plume components in Hawaiian picrites inferred from correlated Os–Pb isotopes. Nature 381: 221–224

Budahn JR, Schmitt RA (1985) Petrogenetic modeling of the Hawaiian tholeiitic basalts: a geochemical approach. Geochim Cosmochim Acta 49: 67–87

Chauvel C, Hofmann AW, Vidal P (1992) HIMU-EM: the French Polynesian connection. Earth Planet Sci Lett 110: 99–119

Chen C-Y, Frey FA, Rhodes JM, Easton RM (1996) Temporal geochemical evolution of Kilauea volcano: comparison of Hilina and Puna basalt. Am Geophys Union Geophys Monogr 95: 161–182

Chen C-Y, Frey FA, Garcia MO, Dalrymple B (1991) The tholeiite to alkalic basalt transition at Haleakala Volcano, Maui, Hawaii: petrogenetic interpretations based on major and trace element and isotope geochemistry. Contrib Mineral Petrol 106: 183–200

Clague DA, Moore JG, Dixon JE, Friesen WB (1995) Petrology of submarine lavas from Kilaueaís Puna Ridge, Hawaii. J Petrol 36: 299–349

Decker RW, Christiansen RL (1984) Explosive eruptions of Kilauea Volcano, Hawaii. In: Explosive volcanism: inception, evolution and hazards. Studies in geophysics. National Academy Press, pp 122–132

Doell RR, Dalrymple GB (1973) Potassium–argon ages and paleomagnetism of the Waianae and Koolau volcanic series, Oahu, Hawaii. Geol Soc Am Bull 84: 1217–1242

Eiler JM, Farley KA, Valley JW, Hofmann AW, Stolper EM (1996) Oxygen isotope constraints on the sources of Hawaiian Volcanism. Earth Planet Sci Lett 144: 453–468

Farley KA (1995) Rapid cycling of subducted sediments into the Samoan mantle plume. Geology 23: 531–534

Feigenson MD, Hofmann AW, Spera FJ (1983) Case studies on the origin of basalt. II. The transition from tholeiitic to alkalic volcanism on Kohala Volcano, Hawaii. Contrib Mineral Petrol 84: 390–405

Frey FA, Rhodes JM (1993) Intershield geochemical differences among Hawaiian volcanoes: implications for source compositions, melting process and magma ascent paths. Phil Trans R Soc Lond A 342: 121–136

Frey FA, Wise WS, Garcia MO, West H, Kwon S-T, Kennedy A (1990) Evolution of Mauna Kea Volcano, Hawaii: petrologic and geochemical constraints on postshield volcanism. J Geophys Res 95: 1271–1300

Frey FA, Garcia MO, Roden MF (1994) Geochemical characteristics of Koolau Volcano: implications of intershield geochemical differences among Hawaiian volcanoes. Geochim Cosmochim Acta 58: 1441–1462

Garcia MO, Rhodes JM, Truesdell FA, Pietruszka A (1996) Petrology of lavas from the Puu Oo eruption of Kilauea Volcano. III. The Kupaianaha episode (1986–1992). Bull Volcanol 58: 359–379

Green TH (1994) Experimental studies of trace-element partitioning applicable to igneous petrogenesis: Sedona 16 years later. Chem Geol 117: 1–36

Gurriet P, Frey FA, Garcia MO (1988) Geochemical heterogeneities within Hawaiian tholeiitic shields: evidence from submarine Mauna Loa lavas. EOS Trans AGU 69 (16): 510

Hart SR (1988) Heterogeneous mantle domains: signatures, genesis and mixing chronologies. Earth Planet Sci Lett 90: 273–296

Harte B, Kirkley MB (1997) Partitioning of trace elements between clinopyroxene and garnet: data from mantle eclogites. Chem Geol 136: 1–24

Hauri EH (1996) Major element variability in the Hawaiian mantle plume. Nature 382: 415–419

Heiken G, Wohletz K (1985) Volcanic ash. University of California Press

Hofmann AW, Feigenson MD, Raczek I (1984) Case studies on the origin of basalt. III. Petrogenesis of Mauna Ulu eruption, Kilauea, 1969–1971. Contrib Mineral Petrol 88: 2435

Hofmann A (1998) Geochemical signatures of gabbro in Hawaiian basalts and other OIB: recycling or assimilation. Program and Abstract volume, GSA Penrose Conference Series, Evolution of Ocean Island Volcanoes, Galapagos, Ecuador, p 41

Ila P, Frey FA (1984) Utilization of neutron activation analysis in the study of geologic materials. Atomkernenergie Kerntechnik 44 (Suppl): 710–716
Kinzler RJ (1997) Melting of mantle peridotite at pressures approaching the spinel to garnet transition: application to mid-ocean ridge petrogenesis. J Geophys Res 102: 853–874
Kurz MD, Kenna TC, Kammer DP, Rhodes JM, Garcia MO (1995) Isotopic evolution of Mauna Loa Volcano: a view from the submarine southwest rift Mauna Loa: a decade volcano. Am Geophys Union Geophys Monogr 92: 289–306
Langenheim VA, Clague DA (1987) Stratigraphic framework of volcanic rocks of the Hawaiian Islands. In: Decker et al. RW (eds) Volcanism in Hawaii. US Geol Surv Prop Pap 1350: 55–84
Lassiter JC, Hauri EH (1998) Osmium-isotope variations in Hawaiian lavas: evidence for recycled oceanic lithosphere in the Hawaiian plume. Earth Planet Sci Lett (in press)
Leeman NP, Gerlach DC, Garcia MO, West HB (1994) Geochemical variations in lavas from Kahoolawe Volcano, Hawaii: evidence from open system evolution from plume-derived magmas. Contrib Mineral Petrol 116: 62–77
Lipman PW, Rhodes JM, Dalrymple GB (1990) The Ninole basalt–-implications for the structural evolution of Mauna Loa Volcano, Hawaii. Bull Volcanol 53: 1–19
Lockwood JPO, Lipman PW (1987) Holocene eruptive activity of Mauna Loa Volcano. US Geol Surv Prop Pap 1350: 509–524
Macdonald GA (1967) Forms and structures of extrusive basaltic rocks. In: Hess HH, Poldervaart A (eds) Basalts: the Poldervaart treatise on rocks of basaltic composition. Wiley, New York, pp 1–61
Multhaup RA, Voss Cl, Souza WR (1989) Subsurface mapping of basalts based on petrographic characterization of cuttings from borehole drilling on Oahu, Hawaii. US Geol Surv Water Res Invest Rep 89-4181: 1–48
Norman MD, Garcia MO (1997) Composition of primitive magmas and source characteristics of the Hawaiian plume: constraints from picritic lavas. In Seventh Annual V.M. Goldschmidt Conference, pp 151–152, LPI contribution no. 921, Lunar and Planetary Institute, Houston, Texas
Norman MD, Garcia MO (1998) Primitive magma compositions and source characteristics of the Hawaiian plume: constraints from tholeiitic picrites. Earth Planet Sci Lett 145: 325–394
Pinkerton H, Sparks RSJ (1976) The 1975 sub-terminal lavas, Mount Etna: a case history of the formation of a compound lava field. J Volcanol Geotherm Res 1: 167–182
Plank T, Langmuir CH (1998) The chemical composition of subducting sediment and its consequences for the crust and mantle. Chem Geol 145: 325–394
Presley TK, Sinton JM, Pringle M (1997) Post-shield volcanism and catastrophic mass wasting of the Waianae Volcano, Oahu, Hawaii. Bull Volcanol 58: 597–616
Rhodes JM (1988) Geochemistry of the 1984 Mauna Loa eruption: implications for magma storage and supply. J Geophys Res 93: 4453–4466
Rhodes JM (1996) Geochemical stratigraphy of lava flows sampled by the Hawaii Scientific Drilling Project. J Geophys Res 101 (11): 729–746
Rhodes JM, Narkiewwicz KP, Garcia MO, Kurz M (1997) The evolution of Mauna Loa Volcano: early picritic lavas. EOS Trans AGU 78 (46): F827
Rhodes JM, Hart SR (1995) Episodic trace element and isotopic variation in historical Mauna Loa lavas. Am Geophys Union Geophys Monogr 92: 263–288
Roden MF, Frey FA, Clague DA (1984) Geochemistry of tholeiitic and alkalic lavas from the Koolau Range, Oahu, Hawaii: implications for Hawaiian volcanism. Earth Planet Sci Lett 69: 141–158
Roden MF, Trull T, Hart SR, Frey FA (1994) New He, Nd, Pb and Sr isotopic constraints on the constitution of the Hawaiian plume: results from Koolau Volcano, Oahu, Hawaii. Geochim Cosmochim Acta 58: 1431–1440
Rowland SK (1987) The flow character of Hawaiian basaltic lavas. PhD, University of Hawaii, 118 pp
Rowland SK, Walker GPL (1987) Toothpaste lava: characteristics and origin of a lava structural type transitional between pahoehoe and aa. Bull Volcanol 49: 631–641
Sobolev A, Hofmann AW, Nikogosian I (1998) Anomalous Sr in melt inclusions from Mauna Loa, Hawaii: fingerprint of recycled gabbro? EOS Trans AGU 79 (17): S345
Staudigel H, Zindler A, Hart SR, Leslie T, Chen C-Y, Clague D (1984) The isotope systematics of a juvenile intraplate volcano: Pb, Nd and Sr isotope ratios of basalts from Loihi Seamount, Hawaii. Earth Planet Sci Lett 69: 13–29
Stearns HT, Vaksvik KN (1935) Geology and groundwater resources of the island of Oahu, Hawaii. Territory of Hawaii, Division of Hydrography Bulletin 1: 1–479
Stille P, Unruh DM, Tatsumoto M (1983) Pb, Sr, Nd and Hf isotopic evidence of multiple sources for Oahu, Hawaii basalts. Nature 304: 25–29
Walker GPL (1986) Koolau dike complex, Oahu: intensity and origin of a sheeted-dike complex high in a Hawaiian volcanic edifice. Geology 14: 310–313
Walker GPL (1987) The dike complex of the Koolau volcano, Oahu: internal structure of a Hawaiian rift zone. In: Volcanism in Hawaii. Decker RW et al. (eds.) US Geol Survey Prof Paper 1350: 961–993
Walker GPL (1989) Spongy pahoehoe in Hawaii: a study of vesicle-distribution patterns in basalt and their significance. Bull Volcanol 541: 199–209
Weaver B (1991) The origin of ocean island basalt end-member compositions: trace element and isotopic constraints. Earth Planet Sci Lett 104: 381–397
Wentworth CK (1951) Geology and ground-water resources of the Honolulu–Pearl Harbor area. Board of Water Supply, City and County of Honolulu, Honolulu, Hawaii, 111 pp
Wentworth CK, Winchell H (1947) Koolau basalt series, Oahu, Hawaii. Bull Geol Soc Am 58: 49–78
Wessel P (1993) Observational constraints on models of the Hawaiian hot spot swell. J Geophys Res 98 (16): 95–104
West HB, Gerlach DC, Leeman WP, Garcia MO (1987) Isotopic constraints on the origin of Hawaiian lavas from the Maui volcanic complex, Hawaii. Nature 330: 216–219
West HB, Garcia MO, Gerlach DC, Romano J (1992) Geochemistry of tholeiites from Lanai, Hawaii. Contrib Mineral Petrol 112: 520–542
Wright TL, Fiske RS (1971) Origin of the differentiated and hybrid lavas of Kilauea Volcano, Hawaii. J Petrol 12: 1–65
Yang H-J, Frey FA, Garcia MO, Clague DA (1994) Submarine lavas from Mauna Kea Volcano, Hawaii: implications for Hawaiian shield stage processes. J Geophys Res 99 (15): 557–594
Yang H-J, Frey FA, Clague D, Garcia MO (1997) Crustal processes in the submarine Hilo Ridge, Hawaii: inferences from phenocryst composition. EOS Trans AGU 78 (46): F644